AD-A083 130 HONEYWELL SYSTEMS AND RESEARCH CENTER MINNEAPOLIS MN F/G 12/1
OPTIMAL LINEAR CONTROL.(U)
DEC 79 C A HARVEY, M G SAFONOV, G STEIN N00014-75-C-0144
UNCLASSIFIED 79SRC87 ONR-CR215-238-4F NL

1 OF 2
AD
A083130

REPORT ONR CR215-238-4F

OPTIMAL LINEAR CONTROL

C.A. HARVEY
M.G. SAFONOV
G. STEIN
J.C. DOYLE

HONEYWELL
SYSTEMS & RESEARCH CENTER
2600 RIDGWAY PARKWAY
MINNEAPOLIS, MINNESOTA 55413

CONTRACT N00014-75-C-0144
ONR TASK 215-238

DECEMBER 1979

FINAL REPORT

PREPARED FOR THE
OFFICE OF NAVAL RESEARCH • 800 N. QUINCY ST. • ARLINGTON, VA. 22217

CHANGE OF ADDRESS

Organizations receiving reports on the initial distribution list should confirm correct address. This list is located at the end of the report. Any change of address or distribution should be conveyed to the Office of Naval Research, Code 211, Arlington, VA 22217.

DISPOSITION

When this report is no longer needed, it may be transmitted to other organizations. Do not return it to the originator or the monitoring office.

DISCLAIMER

The findings and conclusions contained in this report are not to be construed as an official Department of Defense or Military Department position unless so designated by other official documents.

REPRODUCTION

1 ONR

AD-A043 771

UNCLASSIFIED

SECURITY CLASSIFICATION OF THIS PAGE (When Data Entered)

REPORT DOCUMENTATION PAGE

READ INSTRUCTIONS BEFORE COMPLETING FORM

1 REPORT NUMBER: CR215-238-4F	2 GOVT ACCESSION NO.
3 RECIPIENT'S CATALOG NUMBER	
4 TITLE (and Subtitle): Optimal Linear Control	5 TYPE OF REPORT & PERIOD COVERED: Final Report,
6 PERFORMING ORG. REPORT NUMBER: 79SRC87	
7 AUTHOR(s): C.A. Harvey, M.G. Safonov, G. Stein, J.C. Doyle	8 CONTRACT OR GRANT NUMBER(s): N00014-75-C-0144
9 PERFORMING ORGANIZATION NAME AND ADDRESS: Honeywell Systems and Research Center, 2600 Ridgway Parkway, Minneapolis, Minnesota 55413	10 PROGRAM ELEMENT, PROJECT, TASK AREA & WORK UNIT NUMBERS: Program Element: 61153N; Task Area No: RR014-11-84; ONR Task 215-238
11 CONTROLLING OFFICE NAME AND ADDRESS: Office of Naval Research, 800 N. Quincy Street, Arlington, Virginia 22217	12 REPORT DATE: December 1979
	13 NUMBER OF PAGES: 116
14 MONITORING AGENCY NAME & ADDRESS (if different from Controlling Office): RR01411	15 SECURITY CLASS. (of this report): Unclassified
	15a DECLASSIFICATION DOWNGRADING SCHEDULE

16 DISTRIBUTION STATEMENT (of this Report)

RR01411

Approved for public release; distribution unlimited.

12 119

17 DISTRIBUTION STATEMENT (of the abstract entered in Block 20, if different from Report)

18 SUPPLEMENTARY NOTES

19 KEY WORDS (Continue on reverse side if necessary and identify by block number)

Automatic control	Frequency domain	Sectors
Control theory	Multivariable systems	Singular values
Design specifications	Optimal control	Stability
Feedback	Robust control	

20 ABSTRACT (Continue on reverse side if necessary and identify by block number)

This is the final report on a multi-year research program to bridge the gap between modern control theory and practical control system design. The results of the total program are summarized and the last year's results are described in detail. Characterizations of optimal linear controls have been derived, from which guides for selecting the structure of the control system and the weights in the performance index were developed, so that optimal controls meeting conventional design specifications can be designed for

DD FORM 1 JAN 73 1473 EDITION OF 1 NOV 65 IS OBSOLETE

1/0234/9

UNCLASSIFIED

SECURITY CLASSIFICATION OF THIS PAGE (When Data Entered)

20. Abstract (concluded)

conti

single-input systems. For multi-input systems a method of selecting weights for the performance index on the basis of desired closed-loop modal properties and system bandwidth was developed. For such systems it was also found that optimal controls which use state estimators have no guaranteed stability margins, and a method was developed for adjusting the state estimator design so that good margins could be obtained. It was also found that single-loop stability margins in multi-input systems were inadequate measures of robustness, the quality of stability being preserved for a class of perturbations of system characteristics. A new measure of robustness expressed in terms of singular values was developed which is a valid generalization of the concept of stability margins for single-input systems. A method for estimating bounds on system perturbations in terms of singular values associated with parameter uncertainties and unmodeled dynamics, including some forms of nonlinearities, is described in detail in this report. Illustrative examples have been treated in each phase of the program. In this report such an example is presented, demonstrating the use of singular value analysis in design. The final topic described in this report is a method for choosing frequency-dependent design parameters in the Linear Quadratic Gaussian synthesis procedure so that the resulting design meets design specifications on robustness and sensitivity.

FOREWORD

This is the final report on research performed at the Honeywell Systems and Research Center, Minneapolis, Minnesota under Contract N00014-75-C-0144, entitled "Optimal Linear Control." The Scientific Officers for the project were Mr. D.S. Siegel and Mr. R. Von Husen in the Vehicle Technology Division of the Office of Naval Research.

Dr. C.A. Harvey was the Principal Investigator. His co-investigators at Honeywell were Dr. G. Stein, Dr. C.E. Mueller, and Mr. G.L. Hartmann, along with consultants Mr. J.C. Doyle, Dr. E.B. Lee, Dr. M.G. Safonov, and Dr. H.R. Sirisena. Section 3 of this report was written by Dr. Stein, Mr. Doyle, and Dr. Safonov. The other co-workers have contributed to previous reports on the program.

CONTENTS

Section		Page
1	INTRODUCTION	1
2	PROGRAM SUMMARY	3
	Initial Assumptions	3
	Single-Input Results	5
	Multivariable Results	9
	Interpretation of Results Versus Program Objectives	13
3	DETAILS OF LATEST RESULTS	14
	Singular Values and Feedback: Design Examples	15
	Multivariable Robustness Concepts	18
	Example Design Problem	22
	Characterization of L(s)	23
	Trial Controller Designs	28
	Conclusions	35
	Frequency-Domain Analysis of Feedback System Robustnes	36
	Problem Formulation	42
	Robustness of Stability	51
	Bounds on the Overall System's Input-Output Relation T	53
	Discussion	57

CONTENTS (concluded)

Section		Page
	Choice of LQG Cost and Noise Matrixes to Meet Frequency-Domain Robustness and Sensitivity Specifications	58
	The Single-Input-Single-Output (SISO) Case	64
	The Multivariable Case	72
	Conclusion	79
REFERENCES		80
APPENDIX A.	LEMMA A (FREQUENCY-DOMAIN CONICITY TEST)	83
APPENDIX B.	LEMMA B (FREQUENCY-DOMAIN TEST FOR "OUTSIDE" L_{2e}-CONICITY OF INVERSE RELATIONS	87
APPENDIX C.	LEMMA C	91
APPENDIX D.	PROOF OF THEOREM 1	95
APPENDIX E.	PROOF OF THEOREM 2	96
APPENDIX F.	PROOF OF THEOREM 3	102
APPENDIX G.	LEMMA D	105

LIST OF ILLUSTRATIONS

Figure		Page
1	Multivariable Feedback Loop	19
2	Plant with Component Perturbation	20
3	$\sigma(L)$ Bound	25
4	Trial Designs for Pitch Control at Hover	29
5	Trial Designs for Pitch and Vertical Velocity Control	31
6	Transient Responses (Trial 3)	33
7	Canonical MIMO Feedback System	38
8	Interconnected Configuration of Plant	39
9	System with Uncertain Components	43
10	Equivalent System with Uncertain Components	44
11	Component Uncertainty Representation of Uncertain Pole-Zero Locations	46
12	A Feedback Control System	60

SECTION 1

INTRODUCTION

This is the final report on a program aimed at advancing the state-of-the-art of design technology for linear control systems. About 1960, linear optimal control techniques were first developed to provide improved performance of control systems. Practicing control engineers did not recognize any real need for such techniques because the control design problems they faced could readily be treated with previously existing techniques. But the benefits promised by linear optimal control were enticing and the mathematical rigor associated with this formulation of control system synthesis was intriguing to researchers. Publications on this topic dominated the control literature in the ensuing years. The benefits promised by linear optimal control techniques were:

- Optimal performance
- Guaranteed stability
- Integrated multivariable designs
- Computer-automated synthesis

These benefits for a flight control system could be interpreted as providing optimal handling qualities, for example. The guaranteed stability should lead to reduced flight test time and expense. Integrated multivariable design could greatly enhance maneuverability through optimal simultaneous operation of all available control inputs. The computer-automated synthesis could provide inexpensive designs with rapid iteration capability, an extremely attractive feature for integrated vehicle or control-configured vehicle designs.

With few exceptions, these benefits have not been realized. Optimal linear control technology has maintained its research status and control system designers have continued to use conventional design techniques. These conventional design techniques are closely related to design specifications that have evolved through experience with control system behavior. This research program was initiated in 1974 to transform the optimal linear control technology from its research status to a practical design technology. The goal of the research was to bridge the gap between the optimal linear technology and linear control system design practice.

The basic steps proposed to achieve the desired goal were to:

- Formulate the optimization structure and the weight selection procedure in the linear optimal technology so that the resulting control system would meet key conventional design specifications
- Relate conventional design procedures to optimal design procedures to improve their acceptance by practicing design engineers
- Demonstrate the results with authentic examples

The approach taken was to first treat single-input systems and then generalize the results to multi-input systems.

The results obtained in this study are summarized in Section 2. Section 3 presents the technical details of the past year's results.

SECTION 2

PROGRAM SUMMARY

This section presents the initial assumptions and summaries of the results obtained for single-input systems and multi-input systems.

INITIAL ASSUMPTIONS

The primary assumption was that a gap existed between modern control theory as embodied in linear optimal control technology and the design of practical control systems. Modern control theory provided a synthesis method usually formulated in the time domain. The system is represented in this formulation by the linear differential equation

$$\dot{x} = Ax + Bu \tag{1}$$

where x and u denote the state vector and control vector, respectively, and the measurement equation

$$y = Cx \tag{2}$$

where y denotes the vector of measurements. Process noise and sensor noise may be added to these equations. The design specification is expressed in terms of a scalar performance index, which in the deterministic regulator case has the form

$$J = \int_0^\infty (x^T Q x + u^T R u)\, dt \tag{3}$$

The synthesis procedure yields a feedback controller of the form

$$u = -K\hat{x} \tag{4}$$

which stabilizes the system and yields a minimum value for J. If the complete state can be measured, C may be chosen to be the identity, and $\hat{x}$ in Eq. (4) can be replaced by x. Otherwise, $\hat{x}$ denotes an estimate of the state obtained with an observer in the deterministic case and with a Kalman filter in the stochastic case. The gain matrix, K, may be determined by solving an algebraic Riccati equation; various computer algorithms exist for solving such an equation efficiently.

On the other hand, the design of practical control systems used synthesis techniques generally formulated in the frequency domain with the system represented by an input-output relation such as

$$y = G(s)\, u \tag{5}$$

Synthesis was accomplished with the aid of Bode plots, root locus, Nyquist diagrams, etc. The design specifications were expressed in terms of gain and phase margins, bandwidth, high-frequency attenuation, low-frequency gain, response time, peak overshoot, etc.

Each of these technologies had their own strengths and weaknesses. The modern approach treated multi-input systems with ease, could be easily implemented with the aid of a computer, and provided stable controllers. Its weaknesses were that it was not clear how to select the Q and R matrixes or how different observers influenced the system performance, and most importantly that the synthesis procedure was not related to the key design

specifications considered in the practical approach. The strengths of the practical approach were that it was related to key design specifications, was well-understood, and was widely accepted by practicing control system designers. The weaknesses were that it only treated one loop at a time so that it might be conservative, not give the best design, and could be costly in time and money.

Based on this assessment of the gap, we assumed the major step required to bridge the gap was to relate the design parameters in the modern approach to the key design specifications. It was assumed that for this purpose it would suffice to consider only the case in which the complete state could be measured. We also assumed that the existing key design specifications for single-input systems would have direct extensions for multi-input systems.

SINGLE-INPUT RESULTS

Reference 1 presents a detailed description of most of the results obtained for single-input systems. The independent design parameters in the modern approach are the optimization structure, its parameters, and the Q matrix and the scalar R. Choice of the optimization structure is part of the design process. That is, the designer is free to include compensators and integrals of states in the model before applying the optimization procedure. For example, if the system is represented by Eq. (1), a first-order compensator could be added to the model by augmenting Eq. (1) with

$$\dot{u} = -au + av \tag{6}$$

[1] G. L. Hartmann, C. A. Harvey, and C. E. Mueller, "Optimal Linear Control (Formulation to Meet Conventional Design Specs.)," ONR CR215-238-1, Honeywell Systems and Research Center, Minnespolis, Minnesota, March 1976.

and then combining Eq. (1) and (6) into

$$\dot{\tilde{x}} = \hat{A}\tilde{x} + \hat{B}v \tag{7}$$

with $\tilde{x} = (x^T, u)^T$. The optimization can then be performed with respect to a performance index

$$J = \int_0^\infty (\tilde{x}^T \hat{Q} \tilde{x} + v\hat{R}v)\, dt \tag{8}$$

One characterization of optimal linear controls corresponding to Eq. (1), (3), and (4) is that the return difference magnitude is greater than or equal to one for all frequencies. That is,

$$T(-j\omega)\, T(j\omega) \geq 1 \quad \text{for all real } \omega \tag{9}$$

where

$$T(s) = I - G(s) \tag{10}$$

is the return difference, and

$$G(s) = -K(sI - A)^{-1} B \tag{11}$$

is the loop transfer function. This implies that there is a gain margin of at least -6 dB and $+\infty$ dB and phase margin of at least 60 deg at the input u. Also the loop transfer function is asymptotic to a nonzero constant times s^{-1} for large $|s|$. This rate of attenuation of high-frequency inputs may not meet design specifications in many cases. The addition of a compensator as indicated above provides a method for increasing the rate of attenuation. The optimal characteristics hold at the input v, but at the input u the rate

of attenuation of high-frequency inputs is increased from s^{-1} to s^{-2}. The price paid for this increase in high-frequency attenuation rate is a reduction in gain and phase margins at u from those at v. Additional desirable features of the control system may be used in determining the optimization structure. The latest result in this area is presented in the discussion on the choice of performance index parameters to meet frequency domain robustness and sensitivity specifications in Section 3.

For a given optimization structure the optimal controls may be characterized in terms of a set of independent design parameters in the performance index. For an n^{th}-order system there are n such parameters. A convenient set of independent parameters is the weight on control, R, and n - 1 parameters associated with the asymptotic closed-loop eigenvalues which are approached as R tends to zero. For single-input systems the performance index Eq. (4) is equivalent to

$$J = \int_0^\infty (r^T r + Ru^2)\, dt \tag{12}$$

for some scalar

$$r = hx \tag{13}$$

with h denoting a row vector. The performance index Eq. (4) is equivalent to the performance index Eq. (12) in the sense that the optimal control gain matrix is the same. As R tends to zero the closed-loop eigenvalues approach the finite zeros (or their left-half plane images) of the transfer function

$$r/u = h(sI - A)^{-1} B \tag{14}$$

and infinity in a Butterworth pattern of order n - m, where m is the number of finite zeros. With the constraint that the finite zeros lie in the left-half plane, they determine the vector h to within a constant which may be chosen so that the leading coefficient in the numerator of Eq. (14) is one. Then this vector and the parameter R form a convenient characterization of the optimal control. The parameter R is inversely related to the bandwidth and the vector h is related to the root locus parameterized with R.

Design rules based on these characterizations are given in Reference 1. Their use was demonstrated in two illustrative examples there: a jet engine and a flight control system. The only shortcoming was that the compromise between high-frequency attenuation and stability margins associated with the use of a compensator was not clearly delineated. Recognizing that an observer in the deterministic case or a Kalman filter in the stochastic case plays the role of a compensator, we examined the stability margins for a system with such a state estimator in the loop. It was found that for such an optimal control system there is no guaranteed stability margin. This result was reported in References 2 and 3. A method for adjusting the design of observers or Kalman filters was developed so that the stability margins of the closed-loop system with the observer or filter implementation will asymptotically approach those of the full-state feedback implementation as a design parameter tends to infinity. The adjustment procedure is described

---

[2] J.C. Doyle, "Guaranteed Margins for LQG Regulators," IEEE Trans. Automat. Contr., Vol. AC-23, No. 4, August 1978, pp. 756-757.

[3] C.A. Harvey, and J.C. Doyle, "Optimal Linear Control (Characterization and Loop Transmission Properties of Multivariable Systems)," ONR Report No. CR 215-238-3, Honeywell Systems and Research Center, Minneapolis, Minnesota, August 1978.

in References 3 and 4. For the Kalman filter design, this procedure involves adding to the process noise intensity during the filter design an additional matrix multiplied by a scalar parameter. That is, during the design of the filter, the process noise intensity, Q_o, is replaced by

$$Q(q) = Q_o + q^2 B^T V B \tag{15}$$

where V is any positive definite symmetric matrix, q is a scalar parameter, and B is the control coefficient matrix as in Eq. (1). With V fixed, the filter is a function of the parameter, q. And as q tends to infinity, the stability margins of the controller with the filter in the loop as a state-estimator tend to the stability margins of the controller with full-state feedback. Here the trade-off on the design parameter, q, is between the stability margins and the accuracy of the state estimate. These results also hold for multivariable systems.

MULTIVARIABLE RESULTS

The first major result obtained for optimal multivariable control systems was the characterization of the performance index in terms of asymptotic eigenvalues and eigenvectors. This result was reported in References 5 and 6. It is a direct extension of the single-input results and provides a

[4] J.C. Doyle and G. Stein, "Robustness with Observers," IEEE Trans. Automat. Contr., Vol. AC-24, No. 4, August 1979, pp. 607-611.

[5] C.A. Harvey, G. Stein and J.C. Doyle, "Optimal Linear Control (Characterization of Multi-Input Systems)," ONR CR 215-238-2, Honeywell Systems and Research Center, Minneapolis, Minnesota, August 1977.

[6] C.A. Harvey and G. Stein, "Quadratic Weights for Asymptotic Regulator Properties," IEEE Trans. Automat. Contr., Vol. AC-23, No. 3, June 1978, pp. 378-387.

method for selecting the quadratic weights on the basis of desired modal properties. For a multivariable system with n states and m control inputs, the performance index Eq. (3) is equivalent to one of the form

$$J = \int_0^\infty (r^T r + \rho^2 u^T R u)\, dt \tag{16}$$

where r is an m vector

$$r = Hx \tag{17}$$

and ρ is a real scalar parameter. In this case, as ρ tends to zero certain closed-loop eigenvalues approach the finite transmission zeros associated with r and the remainder approach infinity in Butterworth patterns. In addition to this characterization of closed-loop eigenvalues, there is a characterization of the corresponding eigenvectors in terms of H and R in the multi-input case.

In References 5, 6, and 7 it is shown how the m x n matrix H and the m x m matrix R are computed based on desired closed-loop eigenvalues and eigenvectors. This method for selecting weights was demonstrated in two illustrative examples: a flight control system in References 2 and 3, and control of a jet engine in Reference 8.

---

[7] G. Stein, "Generalized Quadratic Weights for Asymptotic Regulator Properties," IEEE Trans. Automat. Contr., Vol. AC-24, No. 4, August 1979, pp. 559-566.

[8] C.A. Harvey and G. Stein, "Linear Multivariable Control Design Based on Asymptotic Regulator Properties," in Alternatives for Linear Multivariable Control, National Engineering Consortium, Inc., Chicago, 1978, pp. 355-367.

The high-frequency attenuation characterization of optimal multivariable controls is also a direct generalization of the single-input case. The attenuation is first-order at each input, and adding a compensator will increase the attenuation order by the difference between the orders of the denominator and numerator of the compensator. Also in this case the price paid for increased order of attenuation is a reduction in stability margins.

It had been assumed at the outset that these characterizations could be related to design specifications. The asymptotic regulator properties could be related to bandwidth and desired modal specifications. The asymptotic filter design procedure could yield single-loop-at-a-time stability margins. But we found that these stability margins were inadequate measures of the robustness of stability with respect to uncertainties. In this regard, valid design specifications for multivariable systems did not exist. This was another major result; examples are given in Reference 3.

Based on this finding, a new method of analyzing robustness of linear multivariable systems was developed in terms of singular values. This method, described in Reference 3, provides a valid generalization of the single-input stability margin concept to multi-input systems. To illustrate this method, consider the unity feedback system with a nominal loop transfer matrix, G(s), and consider a perturbation from the nominal of the form [I + L(s)] G(s). If we assume that G and L are square and rational, that L is stable, that the nominal closed-loop system, $G(I + G)^{-1}$, is stable, and that the determinant of G(s) is not identically zero, then the perturbed system is stable if

$$\underline{\sigma}(I + G^{-1}(s)) > \overline{\sigma}(L(s)) \qquad (18)$$

for all s in the classical Nyquist D-contour. Here $\underline{\sigma}$ and $\overline{\sigma}$ denote minimum and maximum singular values, respectively, and the singular values of a matrix are the square roots of the eigenvalues of the product of the matrix times its complex conjugate transpose. The concept of a stability margin for multi-loop systems may thus be based on the magnitude of the minimum singular value of $I + G^{-1}$. But to be of value, it is necessary to have an estimate, or an upper bound of estimates, of the magnitudes of the maximum singular values of realistically expected perturbations for comparison. In conventional single-input design, such estimates have often evolved from data based on experience and some knowledge about unmodeled dynamics. For example, the 6 dB gain margin is almost a universal specification which covers a wide range of parameter uncertainty, and high-frequency attenuation specifications in flight control systems cover expected resonances of flexure modes and actuator rate limits that are neglected in the design model. There is no such data base for estimates of singular values of expected perturbations in multi-input systems.

The development of methods for estimating and using estimates of uncertainty bounds has been the main subject of our most recent research. The detailed description of the results obtained will be given in Section 3. They may be summarized as follows: To illustrate the role of singular-value analyses in multivariable design, some control law design examples for the CH-47 helicopter were examined. These examples clearly demonstrate the utility of the methodology developed. A methodology was developed for frequency domain analysis of feedback system robustness using sectoricity conditions.

This yields a generalization of the circle stability criterion and can provide tight bounds on the frequency response matrix of the closed-loop system. The final result reported is a characterization of trade-offs between the cost/noise matrixes used in Linear Quadratic Guassian optimal controller synthesis and the robustness properties of the closed-loop system.

INTERPRETATION OF RESULTS VERSUS PROGRAM OBJECTIVES

For single-input systems, the gap between modern control technology and real-world design specifications was bridged. Thus modern control technology can be used for efficient design of good practical control systems. The results provide the framework for the design engineer to judiciously manipulate the design parameters of an optimal control formulation so that design objectives will be satisfied.

For multi-input systems, singular-value analysis provides an underpinning for conventional and modern design technologies which means authentic design specifications for stability margins can now be given (formulated precisely in terms of singular values). Also, design parameters in the optimal theory have been related to conventional design parameters, which means that the choice of design parameters in optimal control technology is no longer a trial-and-error procedure but can be made on the basis of desired closed-loop characteristics.

SECTION 3

DETAILS OF LATEST RESULTS

The results obtained during the final year of the program are presented in this section. To gain insight into the use of singular value analysis in an actual multivariable control system design, the control of the longitudinal motion of the CH-47 helicopter was examined. Single-input and multi-input designs were considered, and these examples provided a good illustration of the applicability of singular value analysis to the design of a system that is robust with respect to actuator rate limits and unmodeled high-frequency dynamics.

The second major topic considered was the frequency-domain analysis of feedback system robustness. This analysis provided two major results: The first is a generalization of the circle stability criterion which yields a quantitative method for characterizing the robustness of a system with respect to component variations. The second is a method for generating tight bounds on the frequency-response matrix of a system based on the nominal system and bounds on perturbations from it. The final topic considered was the choice of cost and noise matrixes, the design parameters in the Linear Quadratic Gaussian (LQG) methodology, so that frequency-domain robustness and sensitivity specifications for the resulting controller would be met. Formal trade-offs were derived and a method is suggested for iteratively adjusting these matrixes to achieve design objectives. Each of these topics is described in detail below.

SINGULAR VALUES AND FEEDBACK: DESIGN EXAMPLES

In this subsection some control law design examples for the CH-47 helicopter are used to explore and illustrate the role of singular value analyses in multivariable design.

Design techniques for linear multivariable control systems have long suffered from the lack of reliable measures of robustness. By robustness we mean an intentionally-designed tolerance for differences between the nominal plant model used for design and the actual plant being controlled. Such differences arise as a result of parameter variations, neglected dynamics, approximated functional relationships, nonlinearities, etc. They are present to some extent in all physical systems. Critical closed-loop properties such as stability must therefore be designed to remain intact in the face of these differences, and key performance variables should exhibit only weak dependence on them.

For single-input single-output systems, the degree to which such tolerance is achieved has been historically (and reliably) measured in terms of the minimum distance of a loop's Nyquist diagram from the so-called critical point (-1, 0) in the complex plane.[9] The familiar concepts of phase margin

---

[9] I. M. Horowitz, Synthesis of Feedback Systems. New York: Academic Press, 1963.

and gain margin are measures of this distance and are often specified as explicit minimum robustness requirements of control loops.[10]

Many attempts have been made to apply these measures of robustness to multivariable systems. A common engineering practice, for example, is to measure gain and phase margins of individual loops one at a time with other loops variously open or closed. More formal methods have been advocated by Rosenbrock,[11] who applies these measures to the inverse Nyquist plots of diagonally dominant systems, and by MacFarlane et al.,[12] who apply them to the eigenvalue (or characteristic loci) plots of multivariable systems. All of these approaches have been shown to be unrealistic in the sense that a lack of tolerance in certain directions goes undetected.[13] In effect, the methods can indicate that all is well with respect to robustness when dangerous sensitivities in fact exist.

---

[10] Background Information and User Guide for MIL-F-94900, Report AFFDL-TR-24-116, Air Force Flight Dynamics Laboratory, January 1975.

[11] H.H. Rosenbrock, Computer-Aided Control System Design. New York: Academic Press, 1974.

[12] A. G. J. MacFarlane and B. Kouvaritakis, "A Design Technique for Linear Multivariable Feedback Systems," International Journal of Control, Vol. 23, No. 6, June 1977, pp. 837-874.

[13] J.C. Doyle, "Robustness of Multivariable Linear Feedback Systems," Proc. IEEE Conf. on Decision and Control, San Diego, California, January 10-12, 1979.

The concept of singular values of matrix transfer functions has recently been applied to overcome this reliability problem. Doyle[13] established a multivariable stability-robustness theorem which guarantees that a stable multivariable control system will remain stable in the face of multiplicative model perturbations whenever the singular values of these perturbations remain appropriately bounded. This result has since been shown by Sandell[14] to be a special case of a general invertability condition for stable perturbed operators. It is also implicit in the recent stability results of Safonov.[15] When it is combined with efficient computational procedures for singular-value decomposition and with tight bounding formulas for the magnitudes of model perturbations, the result appears to provide a valuable new multivariable design tool.

The role which singular value analyses might play in multivariable design will be extended and illustrated by means of some trial control design examples for the longitudinal degrees of freedom of the CH-47 helicopter. In forward flight, this vehicle exhibits coupled pitch attitude and vertical motion dynamics which must be controlled by coordinated actuation of two inputs. This offers a realistic yet manageable design example. We begin the discussions in the next subsection with a quick review of Doyle's stability-robustness result and of some bounding formulas for model

---

[14] N. R. Sandell, "Singular Values and Robustness," Proc. Allerton Conference on Communication, Control, and Computing, Monticello, Illinois, October 1978.

[15] M. G. Safonov, "Robustness and Stability Aspects of Stochastic Multivariable Feedback Design," PhD Dissertation, MIT, September 1977.

perturbations recently developed by Safonov.[16] Specifics of the CH-47 design problem are given in succeeding subsections and various trial designs are then discussed. Conclusions and some open research questions are given in the last subsection. We caution all readers to consider the control laws presented as illustrative only. They are not, and are not intended to be, final 'flight-quality' designs.

Multivariable Robustness Concepts

We consider finite dimensional, linear, time-invariant multivariable feedback loops represented in the frequency domain as shown in Figure 1.† The matrix $G_o(s)$ represents the nominal plant transfer function and L(s) represents a multiplicative perturbation such that the actual plant is given by

$$G(s) = G_o(s)\,[I + L(s)] \tag{19}$$

If L(s) and the nominal closed-loop system, $(I + G_o)^{-1} G_o$, are both stable then the following result holds:

Theorem--The perturbed closed-loop system remains stable for all perturbations L(s) such that

$$\bar{\sigma}[L(s)] < \underline{\sigma}[I + G_o^{-1}(s)] \tag{20}$$

---

†More general systems can be treated with Sandell's[14] and Safonov's[15] generalizations.

[16] M. G. Safonov, "Tight Bounds on the Response of Multivariable Systems with Component Uncertainty," Proc. Allerton Conference on Communication, Control, and Computing, Monticello, Illinois, October 1978.

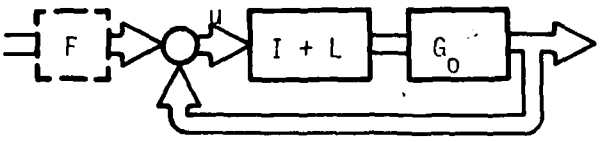

Figure 1. Multivariable Feedback Loop

for all complex frequencies, s, on the classical Nyquist D-contour.† Here the symbols $\bar{\sigma}[A]$ and $\underline{\sigma}[A]$ denote the maximum and minimum singular values of matrix A, respectively, with singular values being defined as the square roots of eigenvalues of A^*A. Equation (20) immediately suggests that the function $\underline{\sigma}[I + G_o^{-1}(s)]$, $s \in D$, provides a reliable measure of multivariable robustness--the bigger $\underline{\sigma}$, the better. Moreover, since this function is equal for $s = \pm j\omega$ and tends to infinity on the infinite segment of the D-contour (at least for all physical systems), it suffices to look at the singular values for real positive frequencies only, that is, the system remains stable if

$$\bar{\sigma}[L(j\omega)] < \underline{\sigma}[I + G_o^{-1}(j\omega)] \tag{21}$$

for all $0 \leq \omega < \infty$.

---

† The D-contour encloses the right-half plane with three segments: 1) $s = j\omega$, $0 \leq \omega < \infty$; 2) $s = Re^{j\theta}$, $R \to \infty$, $-\frac{\pi}{2} \leq \theta \leq \frac{\pi}{2}$; and 3) $s = j\omega$, $-\infty < \omega \leq 0$. It is usually indented to exclude singularities along this path.

This equation calls for nothing more than "generalized Bode gain plots" ($\bar{\sigma}$ and $\underline{\sigma}$ vs. ω) to measure system robustness. We will refer to these plots as sigma-plots for convenience.

In order to use Eq. (21), we must be able to calculate singular values efficiently and be able to characterize realistic perturbations L(s) for complex systems. Numerical procedures for the first requirements are discussed by Laub.[17] The second requirement is satisfied to a substantial degree by the following composite sectoricity results due to Safonov.[16]

Consider the system diagram shown in Figure 2. The matrixes G_o, G_{yv}, G_{eu}, and G_{ey} are nominal transfer functions of our original plant with its block diagram redrawn so that the uncertainties of individual components are all collected into one perturbation matrix: diag $[c_i(s), i = 1, 2, \ldots, N]$.

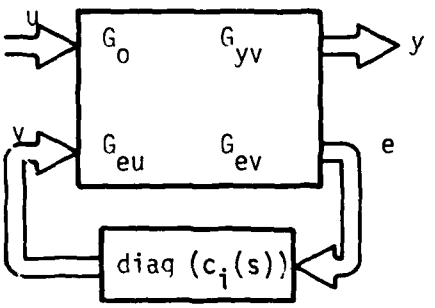

Figure 2. Plant with Component Perturbation

[17] A. J. Laub, "Computational Aspects of Singular Value Decomposition," Proc. Allerton on Communication, Control, and Computing, Monticello, Illinois, October 1978.

The c_i's are nominally zero and are assumed to have known individual bounds

$$|c_i(j\omega)| \leq |r_i(j\omega)| \tag{22}$$

where the r_i's are stable, minimum phase, rational transfer functions. Let $R \triangleq \text{diag}(r_i)$ and let

a) the nominal system be stable, and

b) the matrix $M \triangleq I - G_{ev}^* R^* R G_{ev}$ be uniformly positive for all ω

Then the perturbed system's transfer function matrix will belong to a "conic sector" (a circle in the frequency domain) defined by

$$\bar{\sigma}\left[Q^{\frac{1}{2}}(j\omega)\left(G(j\omega) - G_c(j\omega)\right) P^{-\frac{1}{2}}(j\omega)\right] \leq 1 \text{ for all } \omega \tag{23}$$

with

$$G_c \triangleq G_o + G_{yv} M^{-1} G_{ev}^* R^* R G_{eu} \tag{24}$$

$$Q \triangleq \left[G_{yy} M^{-1} G_{yy}\right]^{-1} \tag{25}$$

$$P \triangleq G_{eu}^* R^* \left[I - R G_{ev} G_{ev}^* R^*\right]^{-1} R G_{eu} \tag{26}$$

Note that Eq. (23)-(26) provide a way to compute bounds for the total perturbation L(s) in Figure 1 from known bounds for individual component elements of the plant.

Example Design Problem

To examine the potential utility of the above concepts in multivariable system design, we will treat a longitudinal-axes design problem for the CH-47 helicopter. This vehicle is a tandem rotor machine whose physical characteristics and mathematical models are given in Reference 18. Control over vertical motions is achieved by simultaneous changes of blade angle-of-attack on both rotors (collective), while pitch and forward motions are controlled by changing blade angle differentially between the two rotors (differential-collective). These blade angle changes are transformed through rotor dynamics and aerodynamics into hub forces which then move the machine.

Our objectives will be to design a command augmentation control law which achieves tight, non-interacting control of the vertical velocity and pitch attitude responses. A small perturbation linearized aircraft model should prove adequate for this purpose and is available.[18] The state vector consists of the vehicle's basic rigid body variables $x = (V, \dot{z}, q, \theta)$ (forward velocity, vertical velocity, pitch rate, pitch angle). Two integrators are appended to achieve integral control of the primary responses, and controls are the collective and differential-collective inputs described above: $u = (c, dc)$. Hence, the design model is

---

[18] A. J. Ostroff, D. R. Downing, and W. J. Road, "A Technique Using a Nonlinear Helicopter Model for Determining Terms and Derivations," NASA Technical Note TN D-8159, NASA-Langley Research Center, May 1976.

$$\dot{x} = Ax + Bu \qquad \text{A, B in Reference 18} \tag{27}$$

$$\dot{x}_5 = -\dot{z} + \dot{z}_{cmd} \tag{28}$$

$$\dot{x}_6 = -\dot{\theta} + \theta_{cmd} \tag{29}$$

The major approximations associated with this model are due to neglected dynamics of the rotors, to neglected nonlinearities in the blade angle actuation hardware, and to variations of the A, B matrixes with operating point (flight condition variations). We will treat modeling errors due to these approximations as sources of the perturbation L(s) in Figure 1 and will attempt to make controllers robust with respect to them.

Characterization of L(s)

In view of the stability-robustness theorem cited earlier, it is justifiable to consider nominal design models to be incomplete if they are not accompanied by estimates of the function $\bar{\sigma}[L(s)]$. (How else can a designer ensure the required degree of robustness?) Such estimates are developed in this section for the model in Eq. (27)-(29).

Perturbations Due to Rotor Dynamics--Elementary dynamic and aerodynamic analyses of rotating airfoils, hinged at the rotor hub, indicate that lift forces will not be transmitted to the hub instantaneously with collective changes in blade angle-of-attack but will appear only when the cone angle of the rotor has appropriately changed. The dynamics of the latter have been shown to be damped second-order oscillations with natural frequency equal to rotor speed and damping determined by somewhat uncertain

aerodynamic effects.[19] Hence, rotor dynamics can be crudely represented by second-order transfer functions

$$g_R(s,\zeta) = \frac{\omega_R^2}{s^2 + 2\zeta\omega_R s + \omega_R^2} \tag{30}$$

with $\omega_R = 25$ and ζ conservatively confined to the range $0.1 \leq \zeta \leq 1.0$. Because collective and differential-collective inputs both involve coning motions of the rotors, one such transfer function will appear in each control channel. Since these dynamics are neglected in Eq. (27), it then follows that any perturbed transfer function matrix computed from Figure 1 will have the form

$$G = G_o(I + L) + G_o \text{ diag } (g_R) \tag{31}$$

hence,

$$L = \text{diag } (g_R - 1) \tag{32}$$

$$\bar{\sigma}[L] = \max_{\zeta} \left| \frac{s^2 + 2\zeta\omega_R}{s^2 + 2\zeta\omega_R s + \omega_R^2} \right| \tag{33}$$

This function was evaluated for a range of $s = j\omega$ values (with brute force maximization over ζ) and is shown by the lower solid line in Figure 3.

---

[19] R.H. Hohenemser and S. Yin, "Some Application of the Method of Multi-blade Coordinates," Journal of American Helicopter Society, July 1972.

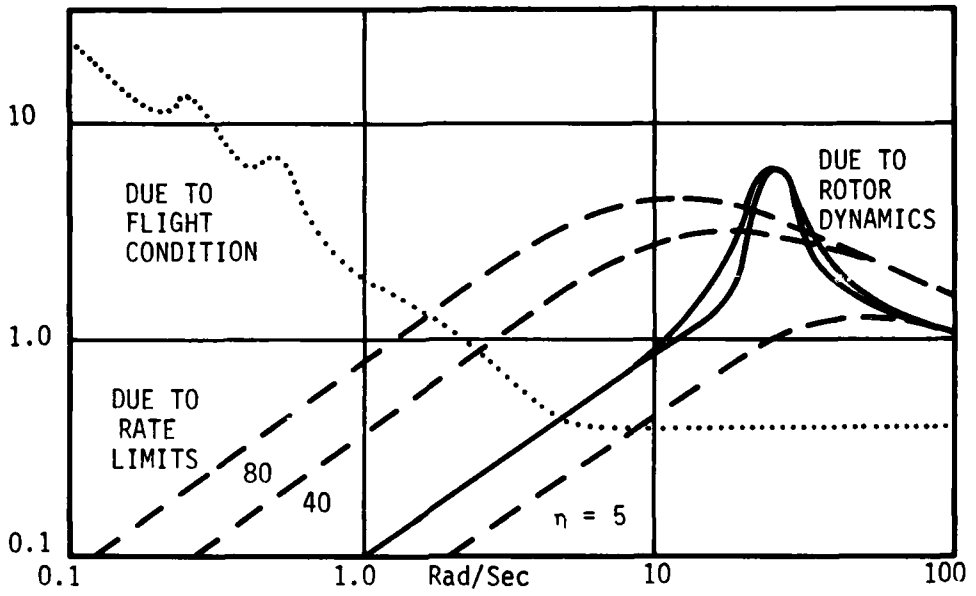

Figure 3. $\sigma(L)$ Bound

An alternate bound for $\bar{\sigma}[L]$ developed from Safonov's formulas, Eq.(23)-(26) is also shown as the upper solid line in Figure 3. In this case, the rotor dynamics are redrawn as in Figure 2, with nominal damping value, $\zeta_o = 0.55$, plus an internal component perturbation, $\delta\zeta$, bounded by

$$|\delta\zeta| \leq |r| \text{ with } r = 0.45 \tag{34}$$

The transfer functions for Figure 2 are

$$\begin{bmatrix} G_o & G_{yv} \\ G_{eu} & G_{ev} \end{bmatrix} = \begin{bmatrix} \omega_R^2 & -2\omega R \\ \omega_R^2 s & -2\omega_R s \end{bmatrix} \left(s^2 + 2\zeta_o \omega_R s + \omega_R^2 \right)^{-1} \tag{35}$$

and according to Eq. (23), the rotor dynamics at each frequency then belong to a circle in the complex plane with center, $\bar{g}_R$, defined by Eq. (24) and radius, $\tilde{g}_R$, given by $\sqrt{p/q}$ with scalars p and q defined by Eq. (25) and (26). Using this circle in Eq. (32) gives the bound

$$\bar{\sigma}[L] \leq |\bar{g}_R - 1| + \tilde{g}_R \tag{36}$$

which is plotted in Figure 3. Note that this "Safonov bound" is slightly more conservative than Eq. (29) because it admits a larger class of damping perturbations--that is, $\delta\zeta$ in Eq. (31) may itself be a dynamical operator.

Perturbations Due to Rate Limits--In addition to the dynamics of rotors, each control channel of the CH-47 also exhibits various nonlinearities which are neglected in the nominal design model. Of these, the rate limit nonlinearity imposes the greatest dynamic constraint on performance, and we consider bounds only for this one effect.

An approximate model for rate limits on the CH-47 is given by

$$\dot{u} = R_{\ell im}\, SAT[94(u_o - u)/R_{\ell im}] \tag{37}$$

where SAT( ) denotes the standard saturation nonlinearity, saturating at ±1. Bounds for this model can be developed with Safonov's procedure by treating the SAT element as an uncertain component. For example, if we are prepared to restrict our system to functions $\zeta(t)$ whose L_∞-norms are less than some multiple of the limit, say

$$||\zeta|_{L^\infty} \leq \eta, \quad \eta \geq 1.0 \tag{38}$$

then

$$SAT(\zeta) = (0.5 + 0.5/\eta) + (\delta c)\zeta \tag{39}$$

with $|\delta c| \leq |r| = 0.5 - 0.5/\eta$

The δc perturbations are nonlinear, of course, and Eq. (23)-(26) do not apply to them as stated. Fortunately, Reference 16 shows that the bounds are still valid for these and other more general perturbations. Hence, the rate limit nonlinearities belong to a conic sector and have a $\bar{\sigma}[L]$ bound analogous to Eq. (37). This bound is plotted in Figure 3 (dashed lines) for several values of the magnitude ratio η. Note that as η becomes large, the bound approaches unity at all frequencies. This is consistent with physical intuition since the effective gain across rate-limited nonlinearities will approach zero for large signal levels.

Perturbations Due to Operating Point--The third major source of model uncertainty is the variation of A, B matrixes with flight condition. Such "component" variation could again be translated into an overall bound for L(s) via Safonov's procedure. In this case, however, the result would be unduly conservative because coefficient variations tend to be highly correlated and are not arbitrary dynamical operators. A more direct way to compute the bound is to solve Eq. (19) for L(s) with known G(s) matrixes and to maximize over a number of representative flight conditions. That is,

$$\bar{\sigma}\, L(j\omega) = \max \bar{\sigma}[G_o^{-1}(j\omega)\, G_i(j\omega) - I] \tag{40}$$

Results of this process are shown by the dotted line in Figure 3. We see the (initially surprising) result that $\bar{\sigma}[L]$ becomes quite large at low frequencies. This happens because the basic helicopter's low-frequency modes are stable at some flight conditions and unstable at others. (Theoretically, $\bar{\sigma}\, G(j\omega)$ will approach infinity for frequencies and flight conditions where these modes cross the $j\omega$-axis.) This means that the perturbations exhibited by our plant are not necessarily stable and, hence, the stability-robustness theorem cited earlier fails to apply. We will see later that stable controllers can still be obtained and that the ability to incorporate unstable L's in a generalized multivariable stability-robustness theory appears to be an important research topic. For the moment, however, our designs will be restricted to individual flight conditions for which the dotted L's in Figure 3 can be disregarded.

Trial Controller Designs

Contemplation of Eq. (21) and the uncertainties given in Figure 3 shows that the stability-robustness theorem basically works by imposing a "multivariable bandwidth" limitation on the feedback loop. Magnitudes of $L(j\omega)$ tend to be large (unity or greater) beyond certain frequencies, requiring G_o^{-1} to be large and consequently G_o to be small. This is most readily illustrated with a single-loop example where plots of the function $\underline{\sigma}[1 + g^{-1}]$ reduce to the inverse closed-loop frequency response, that is,

$$\underline{\sigma}[1 + g^{-1}] = \left|\frac{1 + g}{g}\right| = \left|\frac{1}{g_{cL}}\right| \tag{41}$$

The condition that $\underline{\sigma}[1 + g^{-1}]$ be large then translates directly into the high-frequency "roll-off" requirement commonly imposed on classical control loops.[9] We begin with such an example.

Single-Loop Pitch Attitude Control--The vertical velocity and pitch attitude motions of the nominal CH-47 model at hover uncouple naturally into two non-interacting channels: $(\dot{z}, x_5)$ controlled by (c), and (v, q, θ, x_6) controlled by (dc). The hover flight condition thus offers an attractive single-loop design case. Sigma-plots for several trial pitch-motion controllers for this case are shown in Figure 4. These controllers were all designed with the linear-quadratic methodology (selected largely for convenience) and correspond to the following cost functional:

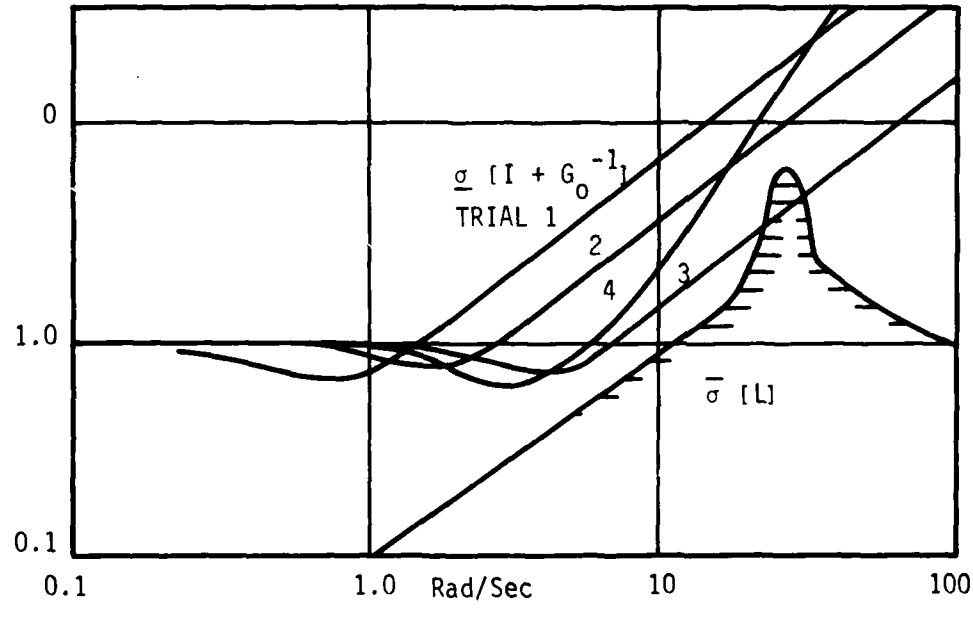

Figure 4. Trial Designs for Pitch Control at Hover

$$J = \int_0^\infty [(57.3\, x_6)^2 + \rho(dc)^2]dt \qquad (42)$$

with ρ = 900., 9.0, 0.09, and 1.0, respectively, for the four trials. (These weighting selections are motivated by the "asymptotic" procedure of Reference 20. They achieve a single slow mode near the origin for forward speed and a third-order (asymptotic) Butterworth pattern for the remaining states.) As expected, bandwidth of these controllers increases with decreasing ρ and eventually violates the stability-robustness constraint imposed by neglected rotor dynamics (for the moment we ignore rate limits and flight condition variations). That this violation actually produces instabilities was verified by computing closed-loop roots of the trial controllers in the presence of the rotor. Trial 3 is unstable! Our options are therefore to restrict bandwidth to approximately Trial 2 or to provide additional roll-off beyond the maximum 20 dB/decade attenuation inherent in LQ-designs.[21] The latter option is illustrated by Trial 4 which uses a ρ value somewhat smaller than Trial 2 but includes a low-pass filter at ω = 12 rad/sec to help avoid the rotor resonance peak. Note that the closed-loop frequency responses† are well-shaped for all pure LQ-trials and that Trial 4 achieves extra bandwidth at the expense of slightly larger M-peaks.

---

† According to Eq. (41), these are given by the sigma-plots of Figure 4 viewed "upside-down."

[20] G. Stein, "Generalized Quadratic Weights for Asymptotic Regulator Properties," IEEE Trans. Auto. Control, Vol. AC-24, No. 4, August 1979, pp. 559-566.

[21] R. E. Kalman, "When is a Linear System Optimal?" Journal of Basic Engineering, Vol. 86, pp. 51-60, 1964.

Multi-Loop Designs--

Maximizing Bandwidth--The beauty of singular values is that the above stability-robustness analyses carry over without change to multivariable systems. This is illustrated in Figure 5 with some trial two-channel designs at a 40-knot forward speed flight condition. These controllers are again of the LQ-type, this time using the cost function

$$J = \int_0^\infty \left[(x_5)^2 + (57.3\, x_6)^2 + \rho_1 (c)^2 + \rho_2 (dc)^2 \right] dt \qquad (43)$$

with (ρ_1, ρ_2) = (10000, 900), (9.0, 9.0), and (1.0, 1.0) for the three trials shown. The distinction between Figures 4 and 5 is that Figure 5 shows two sigma-plots for each trial, corresponding to the two singular values of $(I + G^{-1})$. For stability-robustness, the smaller of these values must

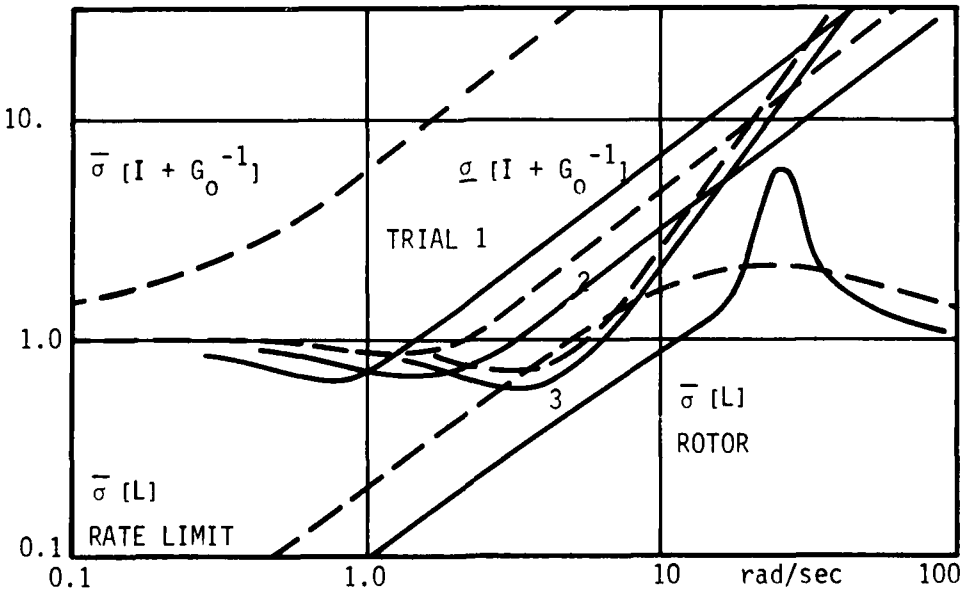

Figure 5. Trial Designs for Pitch and Vertical Velocity Control

fall above the sigma-plot of L at all frequencies. The larger value is unspecified. However, in order to maximize bandwidth "in all directions," it is reasonable to adjust the relative weights (ρ_1, ρ_2) so that the two singular values are approximately equal and then to push them jointly to as high a bandwidth as the $\bar{\sigma}[L]$ plot permits. (For the moment, we again use only neglected rotor dynamics for L.) This design philosophy is incorporated in the three trials of Figure 5. The first trial has low bandwidth and substantial differences between the two singular values. These differences are reduced and bandwidth is increased in the next trial. The third trial serves to maximize bandwidth by using additional roll-off filters in each control channel.

Transient Response--As seen from these trials, singular value analyses appear to offer a convenient way to maximize multivariable bandwidth subject to stability-robustness limitations. The next design step is to achieve reasonable command responses from the resulting feedback loop. One way to do this is to place a command-shaping filter ahead of the loop, as indicated by the dashed box in Figure 1. For feedback loops with integral control on the primary responses, such sophistication is often unnecessary because commands inserted at the integrators (as shown in Eq. (28) and (29)) produce good transients. This is the case here, as evidenced by the responses of Trial 3 to step attitude and step velocity commands shown in Figure 6. Note that the loops are tight, well-damped, and non-interacting, as desired.

Rate Limiting--So far we have ignored model uncertainties due to rate limits. This was done because there is no a priori way to select the

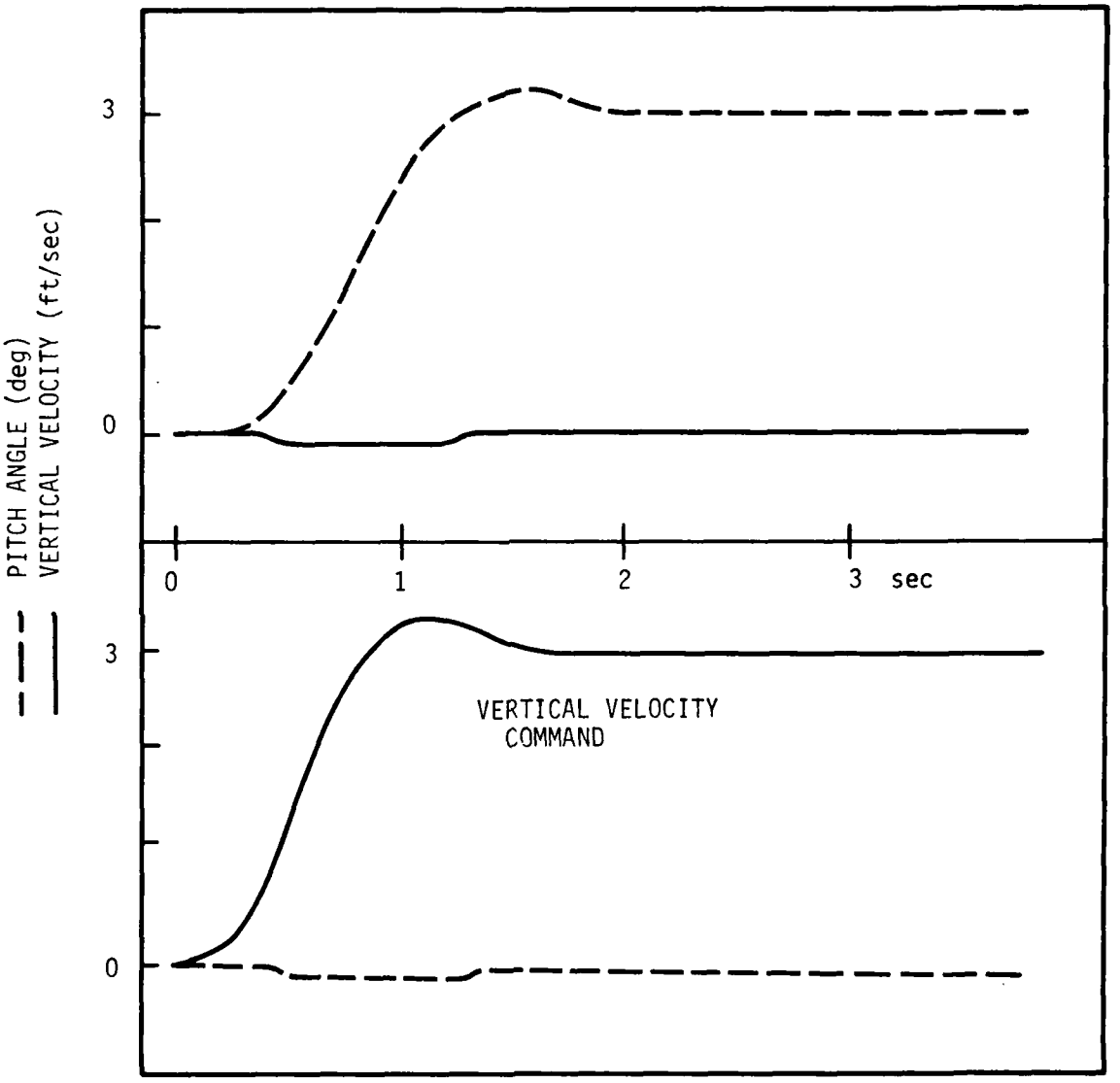

Figure 6. Transient Responses (Trial 3)

parameter η for Figure 3, which is determined by the maximum magnitudes of signals in the closed loop. Clearly, for η sufficiently large, all our trial designs would violate the resulting $\bar{\sigma}[L]$ bound. That such violations actually correspond to instabilities was verified by repeating the transient responses for Trial 3 with progressively larger attitude commands. Unstable behavior occurs for $\theta_{cmd} \geq 18.$ degrees with $\eta \simeq 60.$

In order to improve robustness with respect to rate limits, the following iterative procedure may be used:

1. Assume a signal level limit $\eta \leq \eta_0$.
2. Design $I + G_o^{-1}$ consistent with the resulting $\bar{\sigma}[L]$.
3. Evaluate the actual maximum signal level, η_1, by computing transient responses with worst-case commands and/or initial conditions.
4. If η_1 and η_0 are substantially different, return to step 1 with $\eta_0 = \eta_0 + \epsilon(\eta_1 - \eta_0)$.† Stop otherwise.

An illustration of the first iteration of this procedure is given in Figure 5, where the assumed signal level $\eta_0 = 20.$ (the dashed $\bar{\sigma}[L]$ curve) yields a controller (Trial 2) whose actual signal level is $\eta_1 \leq 0.6$. The associated transient responses are slow but stable. To fine-tune this design, a second iteration might be taken with $\eta_0 = 5.$

Flight Condition Variations--We noted earlier that $\bar{\sigma}[L]$ due to operating point changes becomes quite large at low frequencies because the

† ϵ is at the designer's discretion.

helicopter's slow modes are not stable at all operating points. At intermediate and high-frequency ranges, however, the uncertainty bounds are reasonably small (Figure 3). This suggests that if the loop transfer matrix $G_o(s)$ has sufficient low-frequency gain to stabilize the slow modes under all conditions, then the design might well be stable even though the (sufficient) stability-robustness condition fails. This is in fact the case. Both trial designs 2 and 3 remain stable at eight representative flight conditions ranging from hover to 160-knot forward speed and from +2000 ft/min to -2000 ft/min ascent rates. The intuitive idea underlying this result (sufficiently high low-frequency gain) may well provide needed insight toward a generalized multivariable robustness theory for unstable perturbations.

Conclusions

This subsection has presented several trial control law designs to explore and illustrate the role which singular value analyses might play in multivariable system design. The examples confirm that stability-robustness condition Eq. (20) provides a reliable measure of robustness and they show that this condition offers a natural way to limit multivariable bandwidth during the design process. The bounding formulas Eq. (23)-(26) were seen to be very useful for bounding the functions $\bar{\sigma}[L]$, although for some situations (flight condition variation) they tend to be excessively conservative.

Major weaknesses displayed by the present singular value stability-robustness theory include its inability to handle unstable perturbations and its implicit tendency to limit all loop bandwidths to be consistent with

the worst-case L direction. Although such situations did not arise with the helicopter, it is easy to imagine design problems where some control directions have large L's at low frequencies, hence calling for low bandwidths, while other directions have smaller L's, hence permitting greater bandwidths. It is then unduly conservative to restrict all direction to the slowest case. It is hoped that the examples presented here will motivate further research to overcome these weaknesses.

FREQUENCY-DOMAIN ANALYSIS OF FEEDBACK SYSTEM ROBUSTNESS

A feedback control system design is said to be robust if it is able to meet design specifications despite differences (within a given class) between the nominal plant model used for design and the actual plant. For multi-input-multi-output (MIMO) feedback systems which are subject to bounded perturbations, but which are designed using a linear-time-invariant nominal plant model, frequency-domain "sectoricity" conditions lead to a MIMO generalization of the circle stability criterion, which is found to be useful for ascertaining the robustness of the property of system stability. Moreover, the sectoricity conditions can even provide tight bounds on the frequency response matrix of the closed-loop system.

Besides being able to cope with simple bounded-parameter uncertainty, the results work equally well with perturbations taking the form of time-varying parameters, imprecisely-known component Nyquist-Loci (including so-called "singular perturbations"), and even bounded nonlinearity. The results are indifferent as to whether the perturbations occur at the plant input, at the plant output, or even at internal points in the plant.

In feedback control system design problems, the design specifications usually demand that the system be "robust" against the effects of deviations within specified bounds of the component dynamics from the idealized component models used in designing the system. Such deviations may take the form of unmodeled nonlinearity, incorrect parameter values, time-varying parameters, unmodeled fast modes (including singular perturbations), etc.

A methodology is presented here which, given a MIMO linear-time-invariant (LTI) feedback system design and quantitative bounds on the deviation of the system components from design nominal, enables us to assess robustness in two ways: first, a frequency-domain stability test is presented which allows us to guarantee stability for the entire class of component deviations within the given bounds. This result, which is actually a generalization of the circle stability criterion, provides a method for quantitatively characterizing the robustness of a system against component variations. Second, a method is presented for generating tight quantitative bounds on the feedback system's frequency-response matrix from knowledge of the nominal system dynamics and the given bounds on component deviations from nominal.

While the robustness results which are obtained are quite general in their applicability (they apply even to systems with nonlinear and/or multivariable components) it may prove conceptually helpful to consider a more specific feedback control configuration. Accordingly, we illustrate the practical implications of the results for the "canonical" MIMO feedback system depicted in Figure 7.

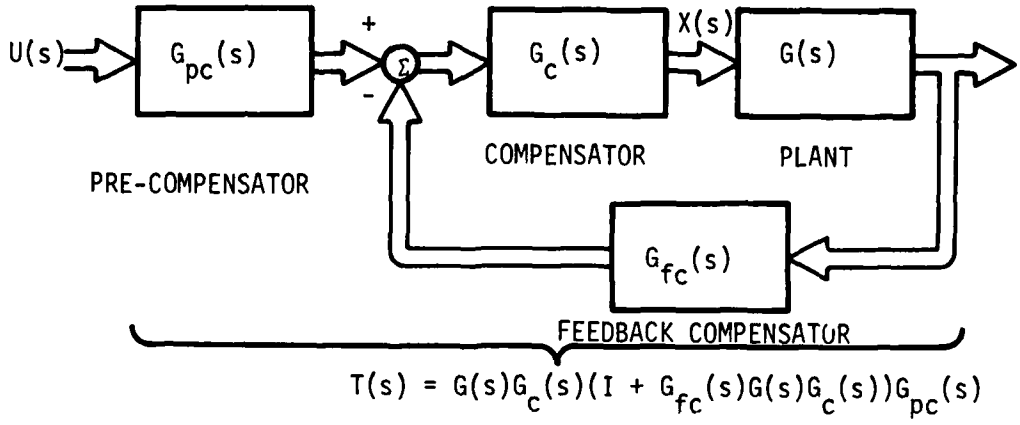

Figure 7. Canonical MIMO Feedback System

The plant G(s) is assumed to consist of the interconnection of single-input single-output (SISO) LTI components $C_i(s) + \delta C_i(s)$ in Figure 8, where

$$C(s) = \begin{bmatrix} C_1(s) & \vdots & \cdots & 0 \\ 0 & C_2(s) & \cdots & 0 \\ \vdots & \vdots & & \\ 0 & \vdots & \cdots & C_N(s) \end{bmatrix} \tag{44}$$

$$\delta C(s) = \begin{bmatrix} \delta C_1(s) & 0 & \cdots & 0 \\ 0 & \delta C_2(s) & \cdots & 0 \\ \vdots & \vdots & & \vdots \\ 0 & \vdots & \cdots & \delta C_N(s) \end{bmatrix} \tag{45}$$

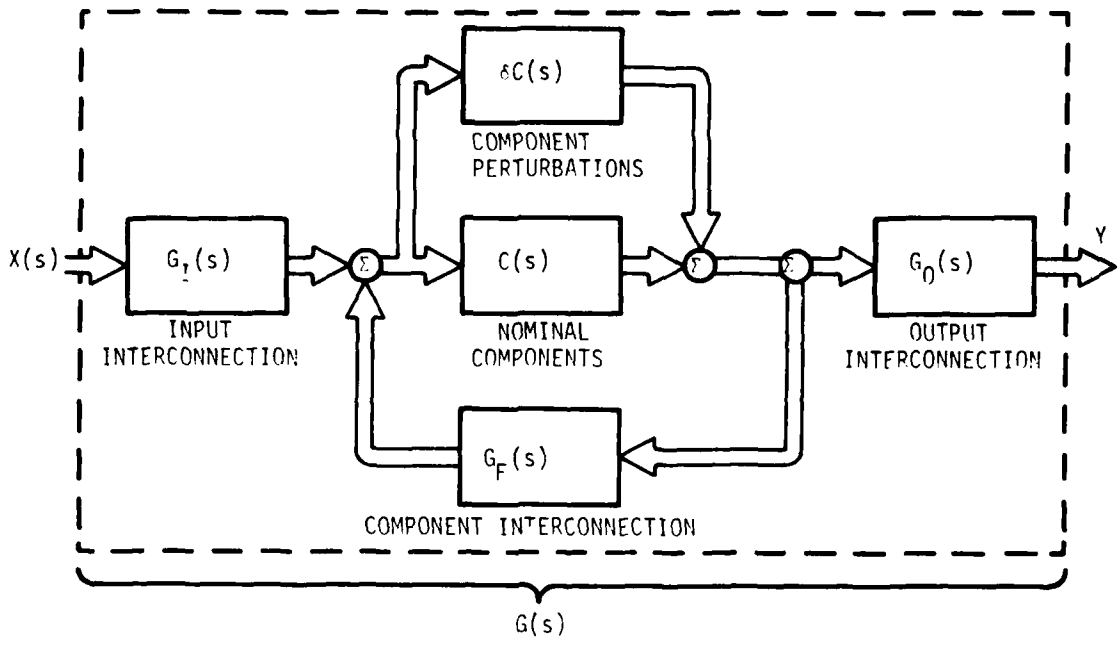

Figure 8. Interconnected Configuration of Plant

It is assumed that the controller matrixes ($G_{PC}(s)$, $G_{FC}(s)$, $G_C(s)$), the plant interconnection matrixes ($G_I(s)$, $G_F(s)$, $G_0(s)$), and the nominal component transfer function matrixes $C_i(s)$ are known. However, the perturbations $\delta C_i(s)$ are assumed to be unknown except that they are open-loop stable and that their frequency responses are bounded in magnitude by the magnitude of given rational transfer functions $R_i(s)$ (with no poles or zeros in $Re(s) \geq 0$):

$$|\delta C_i(j\omega)| \leq |R_i(j\omega)|^2 - \epsilon \tag{46}$$

For some $\epsilon > 0$ and all ω.

Given an operator $\underset{\sim}{A}$, we say that $\underset{\sim}{A}$ is <u>stable</u> if

$$\sup_{\tau} \frac{||\underset{\sim}{A}x||_{\tau}}{||x||_{\tau}} < \infty$$

We say that a feedback system is stable if the operator mapping system input(s) into the system output(s) is stable. We say that an operator is nonanticipative if for any "time" $t_o \in R_+$, the instantaneous output of the operator $(\underset{\sim}{A}x)(t_o)$ is independent of $\{x(t) | t > t_o\}$.

Given an LTI operator with a rational transfer function matrix $A(s) \in C^{nxm}$, we say that $A(s)$ is <u>minimum</u> phase if $A(s)$ has no transmission zeros in $Re(s) \geq 0$; that is, if Rank $(A(s))$ is the same for all s with $Re(s) \geq 0$.

An n x n complex matrix $A(s)$ is para-hermitian if $A^T(-s) = A(s)$.

The following conventions of notation are used in the sequel:

R_+	Non-negative real numbers
x^T, A^T	Transpose of the vector x, the matrix A
L_2	Inner-product space of functions $\underline{x}$: $R_+ \to R^n$ with inner product $\langle x_1, x_2 \rangle_{L_2} = \int_0^\infty x_1^T(t)x_2(t)dt$ and norm $\|x\|_{L_2} = \sqrt{\langle x, x \rangle_{L_2}}$
$A(s)$	Transfer function matrix

x^*, A^*	Complex conjugate of the vector x^T, the matrix A^T
$\underset{\sim}{A}$	Operator mapping R^{n1} valued functions of $t \in R_+$ into R^{n2} valued functions of $t \in R_+$
$L_{2\tau}$	Inner-product space of functions $x:R_+ \to R^n$ with inner-product $\langle x_1, x_2 \rangle_\tau = \int_0^\tau x_1^T(t)x_2(t)dt$ and norm $\|x\|_\tau = \langle x_1, x_2 \rangle_\tau$
$\|x\|_\tau$	(See $L_{2\tau}$ above)
$\langle x_1, x_2 \rangle_\tau$	(See $L_{2\tau}$ above)
L_{2e}	Set of functions $x:R \to R^n$ such that $x \in L_{2\tau}$ for each $\tau < \infty$; that is $L_{2e} = \{x \mid x \in L_{2\tau} \forall \tau \in R_+\}$
$A^{\frac{1}{2}}(s)$	Spectral factor of the full-rank rational para-hermitian matrix $A(s)$ having the properties that $A^{\frac{1}{2}}(s)$ is minimum-phase and has no poles in $Re(s) \geq 0$, and that $(A^{\frac{1}{2}}(-s))^T(A^{\frac{1}{2}}(s)) = A(s)$ (The matrix $A^{\frac{1}{2}}(s)$ always exists for every full-rank rational para-hermitian matrix.)[22]
$A^{\frac{1}{2}}(j\omega)$	$= A^{\frac{1}{2}}(s)\|_{s=j\omega}$ when $A(s) = A(j\omega)\|_{j\omega=s}$

---

[22] D. C. Youla, "On the Factorization of Rational Transfer Function Matrices," IRE Trans. on Information Theory, July, 1961, pp. 172-182.

$\underset{\sim}{A}^{\frac{1}{2}}$	Nonanticipative operator having transfer function $A^{\frac{1}{2}}(s)$; defined for any operator $\underset{\sim}{A}$ (not necessarily causal) whose transfer function A(s) is a full rank para-hermitian matrix
$A \geq 0$	Hermitian matrix A is positive semidefinite
$\underset{\sim}{A}^{*}$	Adjoint of the linear operator $\underset{\sim}{A}$ relative to the inner-product space L_2 (the operator whose impulse response matrix is $W^T(t_1, t_2)$ where $W(t_2, t_1)$ denotes the impulse response matrix of $\underset{\sim}{A}$)
$\bar{\sigma}(A)$	Largest singular value of the matrix A
$\underline{\sigma}(A)$	Smallest singular value of the matrix A
$\underset{\sim}{0}$	Zero operator $\underset{\sim}{0}x = \underline{0}$ for all x
$\underset{\sim}{I}$	Identity operator $\underset{\sim}{I}x = x$ for all x

Problem Formulation

We consider the class of systems which can be represented as a LTI interconnection of N uncertain components, with the system having not more than N outputs. It is assumed that a nominal LTI model $\underline{C}_i(s)$ $(i = 1, \ldots, N)$ is available for each of the N uncertain components but that the actual system components have a perturbed input-output relation $\underline{C}_i(s) + \delta\underset{\sim}{C}_i$. Thus, we are considering the class of systems that can be represented in the form shown in Figure 9.

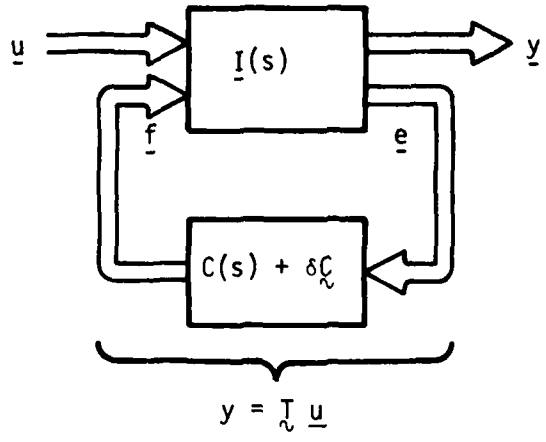

Figure 9. System with Uncertain Components

$$\begin{bmatrix} \underline{y} \\ \underline{e} \end{bmatrix} = I(s) \begin{bmatrix} \underline{u} \\ \underline{f} \end{bmatrix} \tag{47}$$

In this case $Q(s) = 1$, $P(s) = (r(-s)\, r(s))^{\frac{1}{2}}$

$$f = (C(s) + \delta \underset{\sim}{C})\, \underline{e} \tag{48}$$

where

$I(s)$ is the transfer function matrix of the system's LTI internal and external interconnections

$\underline{C}(s) = \text{diag}\,(\underline{C}_1(s), \ldots, \underline{C}_N(s))$

$\delta \underset{\sim}{C} = \text{diag}\,(\delta \underset{\sim}{C}_1, \ldots, \delta \underset{\sim}{C}_N)$

$\underline{e}$ = col $(\underline{e}_1, \ldots, \underline{e}_N)$ where $\underline{e}_i$ $(i = 1, \ldots, N)$ is the i^{th} component's input signal

$\underline{f}$ = col $(\underline{f}_1, \ldots, \underline{f}_N)$ where $\underline{f}_i$ $(i = 1, \ldots, N)$ is the i^{th} component's output signal

$$I(s) = \begin{bmatrix} I_{yu}(s) & I_{yf}(s) \\ I_{eu}(s) & I_{ef}(s) \end{bmatrix}$$

We denote by $\underset{\sim}{T}$ the operator mapping $\underline{u}$ into $\underline{y}$; that is, $\underset{\sim}{T}$ is the overall system's input-output relation

$$\underline{y} = \underset{\sim}{T}\,\underline{u} \tag{49}$$

For analysis, the following equivalent representation of the system (Figure 10) will prove convenient:

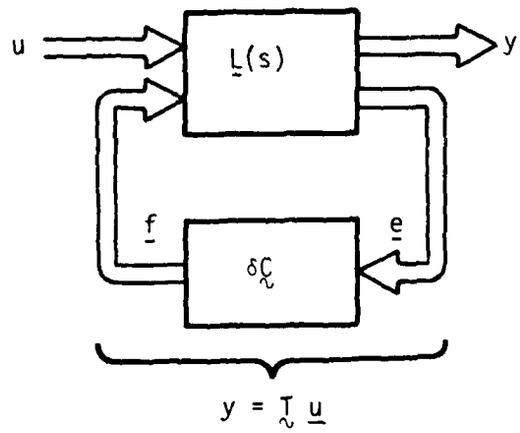

Figure 10. Equivalent System with Uncertain Components

$$\begin{bmatrix} \underline{y} \\ \underline{e} \end{bmatrix} = \underline{L}(s) \begin{bmatrix} \underline{u} \\ \underline{v} \end{bmatrix} \tag{50}$$

$$\underline{v} = \delta \underset{\sim}{C}\, \underline{e} \tag{51}$$

where

$$\underline{v} \triangleq \underline{f} - \underline{C}(s)\, \underline{e} \tag{52}$$

and

$$L \equiv \left[\begin{array}{c|c} L_{yu} & L_{yv} \\ \hline L_{eu} & L_{ev} \end{array}\right] \quad \left[\begin{array}{c|c} I_{yu} + I_{yf} C(I - I_{ef}C)^{-1} I_{eu} & I_{yf}(I - CI_{ef})^{-1} \\ \hline (I - I_{ef}C)^{-1} I_{eu} & I_{ef}(I - CI_{ef})^{-1} \end{array}\right] \tag{53}$$

For example, uncertain pole-zero locations can be analyzed within this framework (see Figure 11).

To keep the mathematics tractable, it is assumed that $\underline{I}(s)$, $\underline{C}(s)$ and, hence, $\underline{L}(s)$ are rational transfer function matrixes. Since it is possible to approximate most interesting systems with non-rational transfer functions arbitrarily closely† by systems with rational transfer functions of sufficiently high degree, this does not appear to be a significant limitation.

The perturbations $\delta \underset{\sim}{C}_i$ are presumed to be uncertain, except that input-output pairs $y = \delta C x$ are assumed to lie within certain "bounding" sets called conic sectors.

---

† By arbitrarily closely we mean that the L_2-norm of the difference in the system's impulse responses can be made arbitrarily small; for stability and transient analysis this is usually a good definition of closeness.

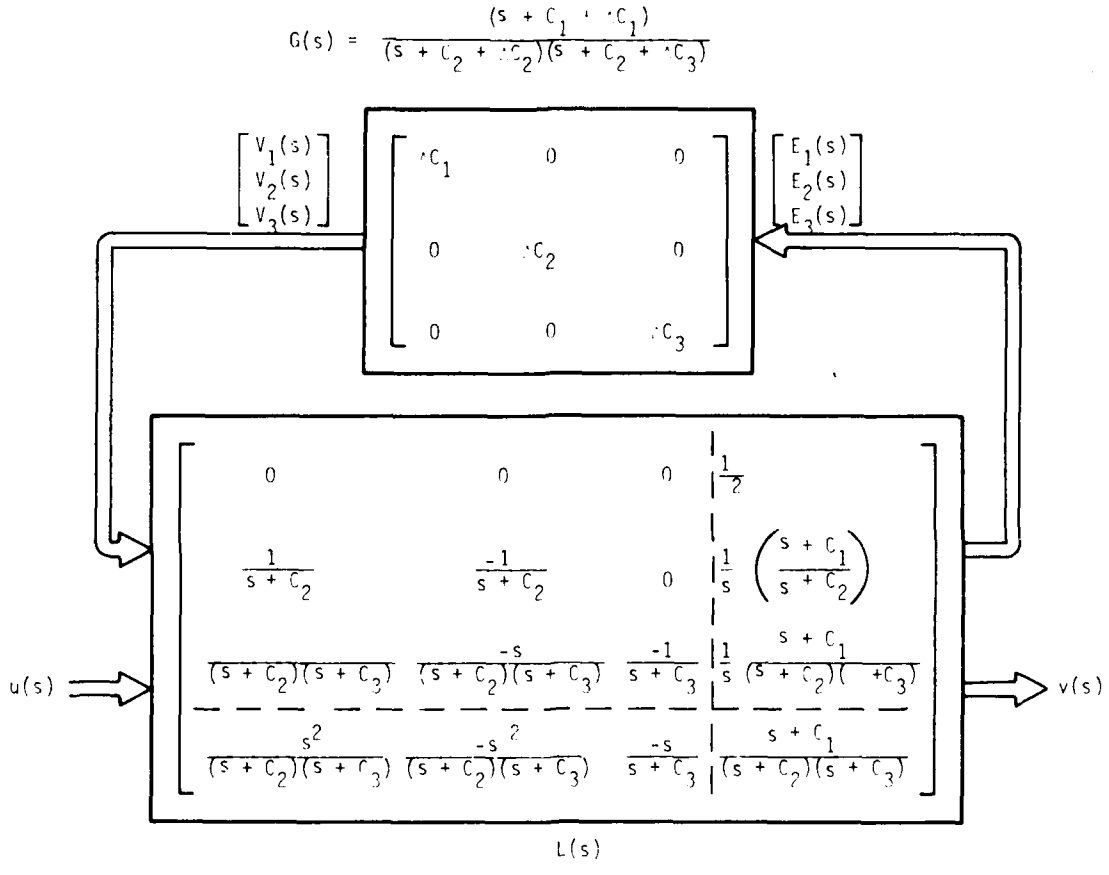

Figure 11. Component Uncertainty Representation of Uncertain Pole-Zero Locations

Definition--Given three operators $\underset{\sim}{C}$, $\underset{\sim}{R}$, and $\underset{\sim}{S}$ mapping into appropriate vector spaces, we define

$$L_{2e}\text{-Cone}\ (\underset{\sim}{C},\ \underset{\sim}{R},\ \underset{\sim}{S}) \triangleq \{(\underline{x},\ \underline{y}) |\ ||\underset{\sim}{S}(\underline{y} - \underset{\sim}{C}\,\underline{x})||_\tau \leq ||\underset{\sim}{R}\,\underline{x}||_\tau \text{ for all } \tau \in R_+\} \subset L_{2e} \times L_{2e} \tag{54}$$

Similarly, we define

$$L_2\text{-Cone}\ (\underset{\sim}{C},\ \underset{\sim}{R},\ \underset{\sim}{S}) \triangleq \{(\underline{x},\ \underline{y}) |\ ||\underset{\sim}{S}(\underline{y} - \underset{\sim}{C}\,\underline{x})||_{L_2} < ||\underset{\sim}{R}\,\underline{x}||_{L_2}\} \subset L_2 \times L_2 \tag{55}$$

If $\underset{\sim}{H}$ is an operator with the property that $\underset{\sim}{H} - \underset{\sim}{C}$ is stable,[†] and if for some $\epsilon > 0$, all $\tau \in R_+$ and all x (with $x \in L_{2\tau}$ for all $\tau \in R_+$)

$$||\underset{\sim}{S}(\underline{y} - \underset{\sim}{C}\underline{x})||_\tau^2 - \epsilon \tag{56}$$

then we say $\underset{\sim}{H}$ <u>strictly inside</u> L_{2e}-Cone $(\underset{\sim}{C},\ \underset{\sim}{R},\ \underset{\sim}{S})$. (57)

Likewise, if for some $\epsilon > 0$ and for all $x \in L_2$

$$||S(y - \underset{\sim}{C}x)||_{L_2}^2 \leq ||Rx||_{L_2}^2 - \epsilon \tag{58}$$

then we say $\underset{\sim}{H}$ strictly inside L_2-Cone $(\underset{\sim}{C},\ \underset{\sim}{R},\ \underset{\sim}{S})$. (59)

[†] We say that an operator $\underset{\sim}{H}$ is stable if $\sup\{||\underline{Hx}||_\tau \div ||x||_\tau \neq 0, \tau \in R_t\} < \infty$.

If Eq. (57) or (58) hold, but with $\epsilon = 0$, then we say "$\underset{\sim}{H}$ inside..." instead of "$\underset{\sim}{H}$ strictly inside..."

(End of Definition)

We remark that in general neither of the two cones, L_{2e}-Cone ($\underset{\sim}{C}$, $\underset{\sim}{R}$, $\underset{\sim}{S}$) and L_2-Cone ($\underset{\sim}{C}$, $\underset{\sim}{R}$, $\underset{\sim}{S}$) is a proper subset of the other.† However, when $\underset{\sim}{H}$, $\underset{\sim}{C}$, $\underset{\sim}{S}$, and $\underset{\sim}{R}$ are stable nonanticipative operators, then Eq. (58) is implied by Eq. (57).

The robustness results reported here assume that associated with each of the uncertain perturbations $\delta\underset{\sim}{C}_i$ ($i = 1, \ldots, N$) are two stable minimum-phase LTI operators $\underset{\sim}{R}_i$ and $\underset{\sim}{S}_i$ with respective rational transfer function matrixes $\underline{R}_i(s)$ and $\underline{S}_i(s)$ such that either

$$\delta\underset{\sim}{C}_i \text{ strictly inside } L_{2e}\text{-Cone}(\underset{\sim}{0}, \underset{\sim}{R}_i, \underset{\sim}{S}_i) \tag{60}$$

or

$$\delta\underset{\sim}{C}_i \text{ inside } L_2\text{-Cone}(\underset{\sim}{0}, \underset{\sim}{R}, \underset{\sim}{S}_i)$$

(where $\underset{\sim}{0}$ denotes the zero operator $\underline{0} \equiv \underset{\sim}{0}\,\underline{x}$)

---

† For example, the L_{2e}-Cone (0, 1, 1) contains unstable functions like $(x, y) = (e^t, e^t)$ which is not in L_2-Cone (0, 1, 1) and L_2-Cone (0, 1, 1) contains functions not in L_{2e}-Cone (0, 1, 1) like $(x, y) = (u_{-1}(t - 1), u_{-1}(t))$ where $u_{-1}(t)$ is the unit step.

We use the notation

$$\underline{\underline{R}}_C(s) \triangleq \text{diag}(\underline{\underline{R}}_1(s), \ldots, \underline{\underline{R}}_N(s))$$

$$\underline{\underline{S}}_C(s) \triangleq \text{diag}(\underline{\underline{S}}_1(s), \ldots, \underline{\underline{S}}_N(s))^{\dagger}$$

$$\underline{\underline{R}}_C \triangleq \text{diag}(\underline{\underline{R}}_1, \ldots, \underline{\underline{R}}_N)$$

$$\underline{\underline{S}}_C \triangleq \text{diag}(\underline{\underline{S}}, \ldots, \underline{\underline{S}}_N)^{\ddagger} \tag{61}$$

It is further assumed that $S_i^*(j\omega)\, S_i(j\omega)$ and $R_i^*(j\omega)\, R_i(j\omega)$ are uniformly positive definite for all ω.

For nonanticipative stable LTI $\delta\underline{\underline{C}}_i$ these conicity conditions are actually equivalent to either of the following two equivalent frequency-domain conditions on the Laplace transform $\delta\underline{\underline{C}}_i(s)$ of the impulse response of $\delta\underline{\underline{C}}$:

1. $R_i^*(j\omega)\, R_i(j\omega) - \delta C_i^*(j\omega)\, S_i^*(j\omega)\, S_i(j\omega)\, \delta C_i(j\omega)$ (62)

   uniformly positive definite for all ω

2. $\bar{\sigma}(S_i(j\omega)\, \delta C_i(j\omega)\, R_i^{-1}(j\omega) \leq 1 - \epsilon$

   for some $\epsilon > 0$ and all ω

---

† For any collection of matrixes $\underline{\underline{A}}_1, \ldots, A_N$, diag $(A_1, \ldots, A_N)$ is the block diagonal matrix.

‡ For any collection of operators $A_1, \ldots, A_N$ the notation $\text{diag}(A_1, \ldots, A_N)$ denotes the operator

$$\underline{\underline{A}} \begin{bmatrix} \underline{x}_1 \\ \vdots \\ \underline{x}_N \end{bmatrix} \triangleq \begin{bmatrix} \underline{\underline{A}}_1 \underline{x}_1 \\ \vdots \\ \underline{\underline{A}}_N \underline{x}_N \end{bmatrix}$$

If additionally $\delta\underline{C}(s)$ is scalar, then these conicity constraints on $\delta\underset{\sim}{C}_i$ are equivalent to the bound

$$|\delta C_i(j\omega)| \leq \frac{|R_i(j\omega)|}{|S_i(j\omega)|} \tag{63}$$

for all ω.

For the canonical LTI feedback control system example of Figures 7 and 8, the matrix L(s) becomes

$$L(s) = \left[\begin{array}{c|c} L_{yu}(s) & L_{yv}(s) \\ \hline L_{eu}(s) & L_{ev}(s) \end{array}\right]$$

$$= \left[\begin{array}{c|c} G_o(s)\, C(s)\, (I + F(s)\, C(s))^{-1} P(s) & G_o(s)\, (I + C(s)\, F(s))^{-1} \\ \hline (I + F(s)\, C(s))^{-1} P(s) & -F(s)\, (I + C(s)\, F(s))^{-1} \end{array}\right]$$

where

$$F(s) = G_F(s) + G_I(s)\, G_C(s)\, G_{FC}(s)$$

$$P(s) = G_{IC}(s)\, G_c(s)\, G_{pc}(s)$$

Notice that $L_{yu}(s) = T(s)$ in the idealized case where $\delta C_i \equiv 0$ for all $i = 1, \ldots, N$.†

---

†These frequency-domain representations of conicity conditions follow from Lemma A (Appendix A), if we take $\underline{u}(t) = e(t) = \underline{E}_o\,(\mathrm{Cos}(\omega t)$ and $\underline{y}(t) = (\delta\underset{\sim}{C}\underline{u})(t) = R_e(\delta\underline{C}(j\omega)\, E_o e^{j\omega t})$.

Robustness of Stability

The following theorem gives sufficient conditions for the overall system $\underset{\sim}{T}$ to be stable.

Theorem 1 (Multivariable Circle Stability Criterion--If

1. $\underset{\sim}{T}$ is stable when $\delta\ \underset{\sim}{C} \equiv \underset{\sim}{0}$ (64)

2. $\underset{\sim}{S}_c^*(j\omega) - \underset{\sim}{R}_c(j\omega)\ \underset{\sim}{L}_{ev}(j\omega)^* \left[\underset{\sim}{R}_c(j\omega)\ \underset{\sim}{L}_{ev}(j\omega)\right]$ (65)

   is positive semidefinite for all ω

Then, the system $\underset{\sim}{T}$ is stable for every collection of perturbations

$$\{\delta\underset{\sim}{C}_i \mid i = 1,\ldots n\}$$

satisfying

$$\delta\underset{\sim}{C}_i \quad \underline{\text{strictly inside}} \quad L_{2e}\text{-Cone}\ (\underset{\sim}{0},\ \underset{\sim}{R}_c,\ \underset{\sim}{S}_c) \qquad (66)$$

$$(i = 1,\ldots N)$$

Proof:

See Appendix D.

Comment:

The condition (65) can be expressed equivalently in a variety of ways in terms of singular values. That is,

1. $\underline{\sigma}(\underline{S}_c^*\underline{S}_c - (\underline{R}_C\ \underline{L}_{ev})^*\ (\underline{R}_c\underline{L}_{ev}) \geq 0$ (67)

2. $\underline{\sigma}\left[(\underline{S}_c\ \underline{L}_{ev}^{-1})^*\ (\underline{S}_C\ \underline{L}_{ev}^{-1}) - \underline{R}_c^*\underline{R}_c\right] \geq 0$ (68)

3. $\underline{\sigma}\,(\underline{S}_c\,\underline{L}_{ev}^{-1}\,\underline{R}_c^{-1}) \geq 1$ (69)

4. $\underline{\sigma}\,(\underline{R}_c\,\underline{L}_{ev}\,\underline{S}_c^{-1}) \leq 1$ (70)

For the canonical LTI feedback control system in Figures 7 and 8 having scalar LTI perturbations δC_i satisfying Eq. (46), Theorem 1 becomes the following.

Corollary 1a--A sufficient condition for the feedback control system of Figures 7 and 8 to be stable for all nonanticipative $\delta \underset{\sim}{C}_i$ ($i = 1, \ldots, N$) satisfying

$$|\delta C_i(j\omega)|^2 \leq |R_i(j\omega)|^2 - \epsilon \tag{71}$$

for some $\epsilon > 0$ and all ω

is

1. the system is stable when $\delta C_i = 0$
2. $\underline{\sigma}\left(C(j\omega) + F^{-1}(j\omega)\,R_c^{-1}(j\omega)\right) \geq 1$ (72)

for all ω, where

$$R_c(s) \triangleq \begin{bmatrix} R_1(s) & 0 & \ldots & 0 \\ 0 & R_2(s) & \ldots & 0 \\ . & & \ldots & . \\ . & & \ldots & . \\ 0 & & \ldots & R_N(s) \end{bmatrix} \tag{73}$$

Proof: From Lemma A,

$$\delta C_i \text{ inside } L_{2e}\text{-Cone } (\underset{\sim}{0}, \underset{\sim}{R}_i, \underset{\sim}{I})$$

where $\underset{\sim}{R}_i$ is the LTI operator whose impulse response is the inverse Laplace transform of $[R_i(-s)\, R_i(s)]$. Condition (72) ensures that Eq. (69) is satisfied, which in turn ensures that Eq. (65) is satisfied. The result follows from Theorem 1.

Bounds on the Overall System's Input-Output Relation T

The following theorem characterizes a conic sector which bounds the input-output relation of the overall system. This in turn can be used to bound the frequency response matrix of the system when all the perturbations $\delta \underset{\sim}{C}_i$ are LTI.

Theorem 2 (Conic Sector Bounds on T)--Suppose for all $i = 1, \ldots, N$ that $\delta \underset{\sim}{C}_i$ inside L_2-Cone $(\underset{\sim}{0}, \underset{\sim}{R}_i, \underset{\sim}{S}_i)$.

Let

$$\underset{\sim}{T}_{NOM} \triangleq \underset{\sim}{L}_{yu} + \underset{\sim}{L}_{yv} (\underset{\sim}{S}_c^* \underset{\sim}{S}_c - \underset{\sim}{L}_{ev}^* \underset{\sim}{R}_c \underset{\sim}{R}_c \underset{\sim}{L}_{ev})^{-1}$$

$$L_{ev}^* R_c^* R_c L_{eu} \tag{74}$$

$$Q_T \triangleq \left(\underset{\sim}{L}_{yv} (\underset{\sim}{S}_c^* \underset{\sim}{S}_c - \underset{\sim}{L}_{ev}^* \underset{\sim}{R}_c^* \underset{\sim}{R}_c \underset{\sim}{L}_{ev})^{-1} \underset{\sim}{L}_{yv}\right)^{-1} \tag{75}$$

$$\underset{\sim}{P}_T = (\underset{\sim}{R}_c \underset{\sim}{L}_{eu})^* \left(I - \underset{\sim}{R}_c \underset{\sim}{L}_{ev} (\underset{\sim}{S}_c^* \underset{\sim}{S}_c)^{-1} (\underset{\sim}{R}_c \underset{\sim}{L}_{ev})\right)^{*-1} (\underset{\sim}{R}_c \underset{\sim}{L}_{eu}) \tag{76}$$

If

a) the overall system T is stable when $\delta C \equiv \underset{\sim}{0}^{\dagger}$ and

b) $S_c^*(j\omega)\, S_c(j\omega) - \left[R_c(j\omega)\, L_{ev}(j\omega)\right]^*\, R_c(j\omega)\, L_{ev}(j\omega)$ (77)

uniformly positive definite for all real ω.

Then

$$\underset{\sim}{T} \text{ inside } L_2\text{-Cone } (\underset{\sim}{T}_{NOM},\ \underset{\sim}{P}_T^{\frac{1}{2}},\ \underset{\sim}{Q}_T^{\frac{1}{2}}) \qquad (78)^{\dagger}$$

Proof: See Appendix E.

The frequency-domain implications of this theorem for LTI $\delta C_i(s)$ are given by the following corollary.

Corollary 2a--Suppose that the δC_i has stable LTI elements satisfying

$$\bar{\sigma}\left(S_i(j\omega)\, \delta C_i(j\omega)\, R_i^{-1}(j\omega)\right) \leq \omega \qquad (79)$$

Let $T_{NOM}(s)$, $\underset{\sim}{P}_T(s)$, and $\underset{\sim}{Q}_T(s)$ be the respective transfer function matrixes of $\underset{\sim}{T}_{NOM}$, $\underset{\sim}{P}_T$, and $\underset{\sim}{Q}$.

---

† We remark that it is possible for the inverses in Q_T to fail to exist. (It happens that the inverse in P_T always exists whenever the inverse in Q_T exists; further the condition (77) ensures that the inverse $(\underset{\sim}{S}_c^* \underset{\sim}{S}_c - \underset{\sim}{L}_{ev}^* \underset{\sim}{R}_c^* \underset{\sim}{R}_c \underset{\sim}{L}_{ev})^{-1}$ exists). The operator $\underset{\sim}{Q}_T$ can fail to exist, however, if $L_{yv}(j\omega)$ does not have full rank at all frequencies ω. The situation would correspond to uncertainty vanishing in certain "vector directions" in the output space in which y lies. This should be regarded as a pathological situation arising from an unrealistic model of the system's uncertainty, somewhat analogous to the situation that arises in Kalman filtering when the measurement noise matrix fails to be invertible.

If

a) the overall system is stable when $\delta \underset{\sim}{C} = \underset{\sim}{0}^{\dagger}$ (80)

b) $\underline{\sigma}\left[S_c(j\omega)\, L_{ev}^{-1}(j\omega)\, R_c^{-1}(j\omega)\right] \geq 1 + \epsilon$ for some $\epsilon > 0$ and all ω (81)

Then for all ω

$$\bar{\sigma}\left[Q_T^{\frac{1}{2}}(j\omega)\,(T(j\omega) - T_{NOM}(j\omega))\,T_T^{\frac{1}{2}}(j\omega)\right] \leq 1 \tag{82}$$

where T(s) denotes the transfer function matrix of the overall system $\underset{\sim}{T}$.

Proof: Follows from Theorem 2 by taking $u(t) = U_o \cos \omega t$ applying Parseval's theorem to Eq. (76) and by observing that the condition

$$P_T - (T - T_{NOM})^* QT\,(T - T_{NOM}) \tag{83}$$
positive semidefinite

is equivalent to the condition

$$\bar{\sigma}\left(Q_T^{\frac{1}{2}}\,(T - T_{NOM})\,P_T^{-\frac{1}{2}}\right) \leq 1 \tag{84}$$

In the case of the canonical feedback control system of Figures 7 and 8, the result of Corollary 2a specializes to the following:

Corollary 2b--Let

$$T_{NOM} = G_o\,(I + CF)^{-1}\,[C - (I - F^* E F)^{-1} F^* E]\,P \tag{85}$$

$$P_T = P^*\,(E^{-1} - F^* F)\,P \tag{86}$$

$$QT = \left(\left[G_o\,(I + CF)^{-1}\right]\,(I - F^* E F)^{-1}\,\left[G_o (I + CF)^{-1}\right]^*\right)^{-1} \tag{87}$$

---

†Note that condition (a) is equivalent to $\underline{L}(s)$ having no poles in $\mathrm{Re}(s) > 0$.

where

$$F = G_F + G_I G_c G_{FC} G_c \tag{88}$$

$$P = G_I G_C G_{PC} \tag{89}$$

$$E = \left[R_C(I + CF)^{-1}\right]^* \left[R_C(I + CF)^{-1}\right] \tag{90}$$

If

a) The system of Figures 7 and 8 is stable when $\delta C_i \equiv 0$ and

b) $\underline{\sigma}\left(\left(C(j\omega) + F^{-1}(j\omega)\right) R_C^{-1}(j\omega)\right) \geq 1 + \epsilon$ (91)

for some $\epsilon > 0$ and all ω.

Then for the feedback control system of Figures 7 and 8 the closed-loop frequency response matrix $T(j\omega)$ is bounded for all ω by

$$\bar{\sigma}\left(Q_T^{\frac{1}{2}}(j\omega)\left(T(j\omega) - T_{NOM}(j\omega)\right) P_T^{-\frac{1}{2}}(j\omega)\right) \leq 1. \tag{92}$$

Proof: Direct substitution into Corollary 2a.

The bounds provided by Theorem 2 and its Corollaries 2a and 2b are optimally tight bounds when the only information available about the perturbations is

$$\delta\underset{\sim}{C} \text{ inside cone } (0, \underset{\sim}{R}, \underset{\sim}{S}) \tag{93}$$

The following theorem makes this statement more precise.

Theorem 3--Let T_{NOM}, $\underset{\sim}{Q}_T$ and $\underset{\sim}{R}_T$ be as in Theorem 2 and suppose that Eq. (76) and (77) hold. Then for every pair $(\underline{u}, \underline{y}) \in L_2$-Cone $(\underset{\sim}{T}_{NOM}, \underset{\sim}{P}_T^{\frac{1}{2}} \underset{\sim}{Q}_T^{\frac{1}{2}})$ there exists a $\delta\underset{\sim}{C}$ inside L_2-Cone $(\underset{\sim}{0}, \underset{\sim}{R}, \underset{\sim}{S})$ such that

$$\underline{y} = (\underset{\sim}{T} + \delta\underset{\sim}{T})\underline{u} \tag{94}$$

Proof: See Appendix F.

Discussion

The main implication of robustness results such as Theorems 1 and 2 is that one can test stability and find conic sector bounds on the response of complicated interconnections of components having unknown-but-bounded uncertainty in their input-output relations. Particularly important is the fact that if the given bounds on component uncertainty are aggregately given as simply

$$\delta\underset{\sim}{C} \text{ strictly inside Cone } (\underset{\sim}{0}, \underset{\sim}{R}_c, \underset{\sim}{S}_c) \tag{95}$$

or the frequency-domain condition

$$\bar{\sigma}\left[\left[\underset{\sim}{S}_c(j\omega)\, \delta\underset{\sim}{C}_i(j\omega)\, \underset{\sim}{R}_c^{-1}(j\omega) \right]\right] \leq 1 \quad \forall\, \omega, \tag{96}$$

Then the bounds on the overall system's input-output relation are optimally tight as a consequence of Theorem 3.

If, for example, we are able to reduce this design specification to a frequency response specification such as

$$\underline{\sigma}\left(Q_{spec}^{\frac{1}{2}}(j\omega)\,(T(j\omega) - T_{spec}(j\omega))P^{-\frac{1}{2}}(j\omega)\right) \geq 0 \tag{97}$$

where

$T_{spec}(j\omega)$ is the desired nominal system frequency response

$Q_{spec}(j\omega)$ and $P_{spec}(j\omega)$ establish bounds on the acceptable deviation between $T(j\omega)$ and $T_{NOM}(j\omega)$

then one can apply standard norm inequalities to the optimally tight bounds of Theorem 2 (or its corollaries) to denote whether this specification Eq. (97) is met. In particular we can show that if, say, Eq. (82) holds, then for any $(T_{spec}, P_{spec}, Q_{spec})$

$$\bar{\sigma}\left(Q_{spec}^{\frac{1}{2}}(j\omega)\left(T(j\omega) - T_{spec}(j\omega)\right)P_{spec}^{\frac{1}{2}}(j\omega)\right) \leq k(j\omega) \tag{98}$$

where

$$k(j\omega) = \frac{\bar{\sigma}\left(P_T^{\frac{1}{2}}(j\omega)\, P_{spec}^{-\frac{1}{2}}(j\omega)\right)}{\underline{\sigma}\left(Q^{\frac{1}{2}}(j\omega)\, Q_{spec}^{-\frac{1}{2}}(j\omega)\right)}$$

$$+ \bar{\sigma}\left(Q_{spec}^{\frac{1}{2}}(j\omega)\left(T_{NOM}(j\omega) - T_{spec}(j\omega)\right) R_{spec}^{-\frac{1}{2}}(j\omega)\right) \tag{99}$$

(The proof of this is straightforward.) Thus the specification Eq. (97) is satisfied if $K(j\omega) \leq 1$ for all ω.

CHOICE OF LQG COST AND NOISE MATRIXES TO MEET FREQUENCY-DOMAIN ROBUSTNESS AND SENSITIVITY SPECIFICATIONS

Formula are presented that characterize the trade-offs between the choice of cost/noise matrixes in Linear Quadratic Gaussian (LQG) stochastic optimal control and resultant feedback systems' "robustness" properties. That is, stability margins, noise response, tracking accuracy, and other

so-called robustness properties that can be characterized in the frequency-domain. An algorithm is described that enables systematic synthesis of feedback compensators to meet frequency-domain inequality specifications on robustness properties by iterative adjustment of LQG cost/noise matrixes. The global convergence properties of the algorithm are discussed.

A great many of the important properties of a LTI feedback control system are directly related to the frequency response of the two matrixes

$$\hat{S}(s) \triangleq (I + \hat{L}(s))^{-1}$$

and $\hat{T}(s) \triangleq I - \hat{S}(s) = \hat{L}(s)\,(I + \hat{L}(s))^{-1}$

where $\hat{L}(s)$ denotes the system's open-loop transfer function matrix resulting when the feedback loops are opened at some specified system node.

For the sake of concreteness, consider the feedback control system of Figure 12, having open-loop transfer matrixes

$$\hat{L}_y(s) = \hat{P}(s)\,\hat{F}(s)$$

$$\hat{L}_u(s) = \hat{F}(s)\,\hat{P}(s)$$

at the y-node and at the u-node, respectively.

Consider $\hat{S}_y$ and $\hat{T}_y$: The matrix $\hat{T}_y$ is the closed-loop system transfer matrix. That is,

$$\hat{y} = \hat{T}_y \hat{r}$$

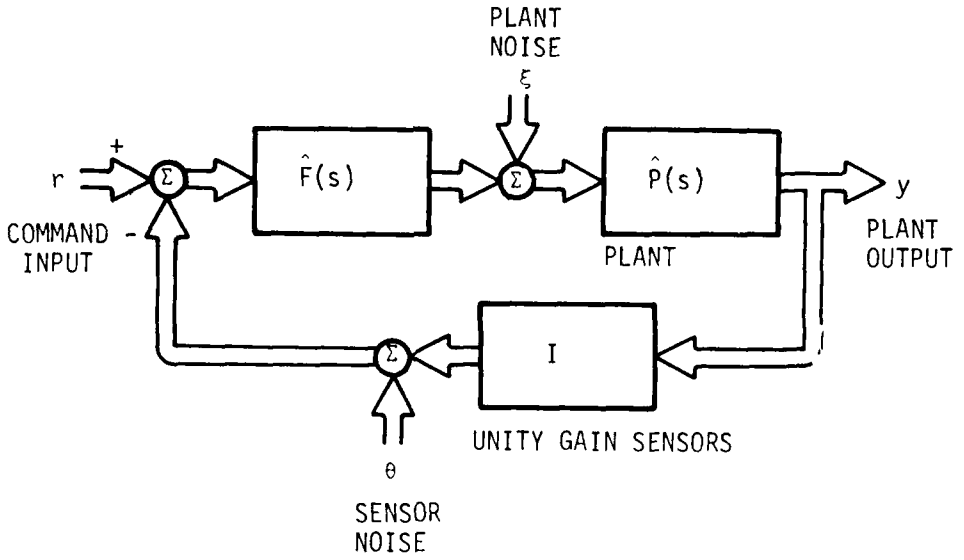

Figure 12. A Feedback Control System

and the closed-loop tracking error is

$$\hat{e} = \hat{S}_y \hat{r}$$

the poles of $\hat{T}_y(s)$ (or, equivalently, the poles of $\hat{S}_y(s)$) are the closed-loop system's poles. The matrix $\hat{S}_y(j\omega)$ is a natural multivariable generalization of the classical Bode sensitivity function characterizing the sensitivity of the system output $\hat{Y}(j\omega)$ to small variations in $\hat{L}_y(j\omega)$. The matrix $\hat{T}_y(j\omega)$ extends to this multivariable feedback configuration the Bode sensitivity function for small variations in the sensor gains. The singular values of

$\hat{T}_y(j\omega)$ characterize the system stability margins[13, 23] (gain and phase margin) at the y-node. The respective sensitivities of $\hat{y}$ to sensor noise, $\hat{\theta}$, and to plant noise, $\hat{\xi}$, are proportional to $\hat{T}_y(j\omega)$ and $\hat{S}_y(j\omega)$. Thus, closed-loop poles, sensitivities of $\hat{y}$ to noise and parameter variations, stability margins at the y-node, and even closed-loop response and tracking error are all directly related to $\hat{S}_y$ and $\hat{T}_y$. Sensitivities and stability margins at the u-node are similarly related to $\hat{S}_y$ and $\hat{T}_u$ which, when $\hat{P}(s)$ exists, are completely determined by $\hat{S}_y$ and $I-\hat{S}_y$ through the relations

$$\hat{S}_y = \hat{P}\,\hat{S}_u\,\hat{P}^{-1}$$

$$I - \hat{S}_y = \hat{P}(I - \hat{S}_u)\,\hat{P}^{-1}$$

It follows that synthesis of a feedback controller to meet specifications regarding pole locations, sensitivities to noise and parameter variations, and stability margins is equivalent to designing $\hat{F}(s)$, to "shape" the matrixes $\hat{S}$ and $I - \hat{S}$ associated with some particular system node.

---

[23] M. G. Safonov and M. Athans, "A Multiloop Generalization of the Circle Stability Criterion," Proc. Asilomar Conference on Circuits, Systems and Computers, Pacific Grove, California, November 6-8, 1978.

The purpose of this subsection is to describe how the frequency response quantities $\hat{S}(j\omega)$ and $\hat{T}(j\omega)$ may be systematically shaped to meet inequality constraints on $||\hat{S}||$ and $||\hat{T}||$ by iterative adjustment of frequency-dependent cost and noise-intensity matrixes in the LQG optimal control problems.[24-26]

The subsection is organized as follows: 1) notation is described, 2) the use of LQG in single-loop feedback synthesis is described in depth, followed by 3) the more complicated multiloop case, and 4) the conclusions are presented.

Notation

x^T, A^T denote the transpose of x, A

x^*, A^* denote the complex-conjugate of x^T, A^T

Fourier and Laplace transforms and frequency-responses and transfer functions are denoted with a circumflex accent: $\hat{x}(s)$, $\hat{A}(j\omega)$, $\hat{B}(s)$, $\hat{Q}(-s^2)$, etc. Where no confusion can result, the arguments involving $j\omega$ and s are suppressed.

$\hat{x}_*(s)$, $\hat{A}_*(s)$ denote $\hat{x}^T(-s)$, $\hat{A}^T(-s)$

---

[24] M. Athans, "The Role and Use of the Stochastic Linear-Quadratic-Gaussian Problem in Control System Design," IEEE Trans. on Automatic Control, Vol. AC-16, 1971, pp. 529-552.

[25] D. C. Youla, et al., "Modern Wiener-Hopf Design of Optimal Controllers Part I: The Single-Input-Output Case," IEEE Trans. on Automatic Control, Vol. AC-21, 1976, pp. 3-13.

[26] D. C. Youla, et al., "Modern Wiener-Hopf Design of Optimal Controllers--Part II: The Multivariable Case," IEEE Trans. On Automatic Control, Vol. AC-21, 1976, pp. 319-338.

Note that

$$\hat{x}_*(j\omega) = \hat{x}^*(j\omega) \quad \forall\ \omega$$

$$\hat{A}_*(j\omega) = \hat{A}^*(j\omega) \quad \forall\ \omega$$

for all $(\hat{x}, \hat{A})$ that are Laplace or Fourier transforms of real-valued functions.

The notation $\sigma_j(A)$ $(i = 1, 2, 3, \ldots)$ is used to denote the singular values of A ordered such that

$$\sigma_1(A) \geq \sigma_2(A) \geq \sigma_3(A) \geq \ldots$$

The singular values of A are the square-roots of the eigenvalues of A*A (and also AA*). Orthonormal eigenvectors $u_i(i = 1, \ldots)$ of AA* are <u>left singular vectors</u> of A; analogously orthonormal eigenvectors $v_i(i = 1, \ldots)$ of A*A are <u>right singular vectors</u> of A. Note that

$$A = \sum \sigma_i u_i v_i^*$$

The largest singular value of A is denoted $\sigma_{max}(A)$.

$\delta_{-1}(\cdot)$ denotes the unit step function,

$$\delta_{-1}(\alpha) = \begin{cases} \alpha, & \text{if } \alpha \geq 0 \\ 0, & \text{if } \alpha < 0 \end{cases}$$

If the matrix $\hat{Q} = \hat{Q}_*$ is rational and if $\hat{Q}(j\omega)$ is positive semidefinite for all ω, we denote by $\hat{Q}^{\frac{1}{2}(r)}$ and $\hat{Q}^{\frac{1}{2}(\ell)}$ any stable minimum-phase spectral factors of $\hat{Q}$ satisfying

$$\hat{Q} = (\hat{Q}^{\frac{1}{2}(r)})_* \; (\hat{Q}^{\frac{1}{2}(r)}) = (\hat{Q}^{\frac{1}{2}(\ell)}) \, (\hat{Q}^{\frac{1}{2}(\ell)})_*$$

such spectral factors always exist. Note that if $\hat{Q}$ is a 1 x 1-matrix, then $\hat{Q}^{\frac{1}{2}(r)} = \hat{Q}^{\frac{1}{2}(\ell)}$ and we may write simply $\hat{Q}^{\frac{1}{2}}$ without ambiguity.

The Single-Input-Single-Output (SISO) Case

Consider the problem of designing a stabilizing proper rational SISO feedback compensator

$$\hat{u}(s) = \hat{F}(s) \left(\hat{r}(s) - \hat{y}(s)\right) \tag{100}$$

for the strictly proper rational SISO plant

$$\hat{y} = \hat{P}(s) \cdot \hat{u}(s) \tag{101}$$

subject to the frequency-domain constraints

$$\hat{\rho}_1 \cdot |\hat{S}|^2 < 1, \; \forall\omega \tag{102}$$

$$\hat{\rho}_2 \cdot |\hat{T}|^2 < 1, \; \forall\omega \tag{103}$$

where $\hat{\rho}_1$ and $\hat{\rho}_2$ are real-valued uniformly bounded, uniformly positive functions of ω^2 with $\lim \hat{\rho}_1(\omega^2) < 1$ and where $\omega \to \infty$

$$\hat{S} \triangleq 1 - \hat{T} = (1 + \hat{P}\,\hat{F})^{-1} \tag{104}$$

The variables $\hat{\rho}_1$ and $\hat{\rho}_2$ may be selected to reflect design specifications on such things as stability margins, sensitivity to plant and sensor noise and/or parameter variations, closed-loop tracking error, frequency response, resonance peak, and other measures of system performance related to $|\hat{S}|$ and $|\hat{T}|$. However, we will not dwell on how to choose $\hat{\rho}_1$ and $\hat{\rho}_2$, but rather will be concerned solely with the problem of synthesizing a stabilizing feedback F to satisfy Eq. (102) and (103) for given $\hat{\rho}_1$ and $\hat{\rho}_2$.

We make no a priori assumption that there exists a stabilizing $\hat{F}(s)$ that meets the specifications (102) and (103). However, when $\hat{F}(s)$ does exist, then the problem is equivalent to the optimization

$$\inf J_1(\hat{S}) \qquad (105)$$
$$\hat{S} \in S$$

where

$$J_1(\hat{S}) = \frac{1}{2\pi} \int_{-\infty}^{\infty} \left[\hat{W}_1 \cdot \hat{M}_1 \cdot |\hat{S}|^2 + \hat{W}_2 \cdot \hat{M}_2 \cdot |1 - \hat{S}|^2\right] d\omega \qquad (106)$$

$S \triangleq \{S \mid \hat{S} = (1 + PF)^{-1}$ F proper and rational;

$\hat{F}\,\hat{P}$ has no pole-zero cancellations in $\mathrm{Re}(s) \geq 0$;

$\hat{S}$ has no poles in $\mathrm{Re}(s) \geq 0\}$

$$W_1(\hat{S}) \triangleq \delta_{-1}(\hat{\rho}_1 \cdot |\hat{S}|^2 - 1) \qquad (107)$$

$$W_2(\hat{T}) \triangleq \delta_{-1}(\hat{\rho}_2 \cdot |\hat{T}|^2 - 1) \qquad (108)$$

where $\hat{M}_1$ and $\hat{M}_2$ are specified real-valued positive functions of ω. Note that $J_1(\hat{S}) = 0$ if and only if (102) and (103) are satisfied, otherwise

$J_1(\hat{S}) > 0$. Furthermore, if $J_1(\hat{S}_o) = 0$ for some $\hat{S}_o \in S$, then J_1 has no local minimum $\hat{S}_1 \in S$ for which $J_1(\hat{S}) > 0$ (Lemma D, Appendix G). So whenever there exists an $\hat{S}_o$ such that (102) and (103) are satisfied, then associated with every $S_1 \in S$ at which $J_1(\hat{S}_1 > 0$ and with every $\epsilon > 0$ there is an $S_2 \in S$ with $|S_2 - S_1| \leq \epsilon \; \forall \omega$ such that $J_1(\hat{S}_2) < J_1(\hat{S}_1)$. (109)

Thus, if one can find an algorithm that generates such an $\hat{S}_2$ for every such $\hat{S}_1$, then subject to the additional technical condition that the amount of decrease is for all $\hat{S}_1$ uniformly bounded below by some continuous non-negative strictly increasing function $\phi(J_1(\hat{S}_1))$, the algorithm when applied iteratively converges to an $\hat{S} \in S$ such that (102) and (103) are satisfied. LQG stochastic optimal control theory is the basis for such an algorithm.

The LQG theory[24-27] provides a method for solving the superfically unrelated optimization problem

$$\min_{\hat{F} \in S} E\left(\frac{1}{2\pi} \int_{-\infty}^{\infty} (\hat{y}_* \hat{Q} \hat{y} + \hat{u}_* \hat{R} \hat{u}) \, d\omega\right)$$

subject to

$$\hat{y} = \hat{P} \cdot (\hat{u} + \hat{\xi})$$

$$\hat{u} = -\hat{F} \cdot (\hat{y} + \hat{\theta})$$

---

[27] U. Shaked, "A General Transfer Function Approach to the Steady-State Linear Quadratic Gaussian Stochastic Control Problem," International Journal of Control, Vol. 24, 1976, pp. 771-800.

where $(\hat{\xi}, \hat{\theta})$ are independent stochastic processes having respective power spectra $(\hat{\Xi}, \hat{\theta})$. The connection between LQG theory and the present problem becomes somewhat more transparent if we observe that the above LQG optimization problem is equivalent to the unconstrained optimization problem (see Reference 25).

$$\min_{\hat{S} \in S} J_2(\hat{S}) \tag{110}$$

where

$$J_2(\hat{S}) = \frac{1}{2\pi} \int_{-\infty}^{\infty} \left\{ \hat{Q}\, \hat{\Xi} \cdot |\hat{P}|^2 \cdot |\hat{S}|^2 + (\hat{R} \cdot \hat{\theta} \cdot |\hat{P}|^{-2} + \hat{R} \cdot \hat{\Xi} + \hat{Q}\, \hat{\theta}) \cdot |1 - \hat{S}|^2 \right\} dw \tag{111}$$

where $(\hat{Q}, \hat{\Xi}, \hat{R}, \theta)$ and their inverses are specified proper rational functions of $-s^2$.

The connection between the LQG problem and the optimization (105) can be further clarified as follows: Let $(\hat{Q}, \hat{\Xi}, \hat{R}, \theta)$ be arbitrary and let $\hat{S}_o$ denote the resulting minimum of J_2. Now suppose that we perturb $(\hat{Q}, \hat{R})$ by making the substitutions

$$\hat{Q} \leftarrow \hat{Q} + \epsilon \Delta \hat{Q} \tag{112}$$

$$\hat{R} \leftarrow \hat{R} + \epsilon \Delta \hat{R} \tag{113}$$

where

$$\Delta \hat{R} = \Delta \hat{R}_1 + \Delta \hat{R}_2 \tag{114}$$

$$\Delta\hat{R}_2 = - |\hat{P}|^2 \cdot (\Delta\hat{Q} \cdot \hat{\theta} + \Delta\hat{R}_1 \cdot \hat{\Xi}) / (|\hat{P}|^2 \hat{\Xi} + \hat{\theta}) \tag{115}$$

$$1 > \epsilon > 0 \tag{116}$$

The change in functional $J_2(\hat{S})$ is for any fixed $\hat{S}$ given by

$$\Delta J_2(\hat{S}) = \epsilon \frac{1}{2\pi} \int_{-\infty}^{\infty} \left\{ \Delta\hat{Q}\, \hat{\Xi}\, |\hat{P}|^2 \cdot |\hat{S}|^2 + \left((\Delta\hat{R}_1 + \Delta\hat{R}_2) \cdot |\hat{P}|^{-2} \cdot |\hat{P}|^2 \cdot \hat{\Xi} + \hat{\theta} \right) + \Delta\hat{Q}\, \hat{\theta} \cdot |1 - \hat{S}|^2 \right\} d\omega \tag{117}$$

$$= \epsilon \frac{1}{2\pi} \int_{-\infty}^{\infty} \left[\Delta\hat{Q} \cdot \hat{\Xi} \cdot |\hat{P}|^2 \cdot |\hat{S}|^2 + \Delta\hat{R}_1\, \hat{\theta}\, |\hat{P}|^{-2} \cdot |1 - \hat{S}|^2 \right] d\omega \tag{118}$$

So, if we choose

$$\hat{M}_1 = \hat{\Xi} \cdot |\hat{P}|^2 \tag{119}$$

$$\hat{M}_2 = \hat{\theta} \cdot |\hat{P}|^{-2} \tag{120}$$

$$\Delta\hat{Q} = W_1(\hat{S}_o) \triangleq \delta_{-1} (\hat{\rho}_1 \cdot |\hat{S}_o|^2 - 1 \tag{121}$$

$$\Delta\hat{R}_1 = W_2(\hat{T}_o) \triangleq \delta_{-1} (\hat{\rho}_2 \cdot |1 - \hat{S}_o|^2 - 1) \tag{122}$$

then

$$\Delta J_2(\hat{S}) = \left(\frac{\epsilon}{2\pi}\right)\int_{-\infty}^{\infty} \hat{W}_1(\hat{S}_o)\cdot \hat{M}_1 \cdot |S|^2 + \hat{W}_2(\hat{T}_o)\cdot \hat{M}_2 \cdot |\hat{T}|^2 \, d\omega$$

$$= \epsilon\, J_1(\hat{S}) + \left(\frac{\epsilon}{2\pi}\right)\int_{-\infty}^{\infty} \Big\{ (W_1(\hat{S}_o) - W_1(\hat{S})\cdot M_1 |\hat{S}|^2$$

$$+ (W_2(\hat{T}_o) - W_2(\hat{T}))M_2 |\hat{T}|^2 \Big\} d\omega \qquad (123)$$

Thus, adding the $(\Delta\hat{Q}, \Delta\hat{R})$ terms in the LQG optimization adds a penalty in $J_2(\hat{S})$ for $J_1(\hat{S})$ plus a small penalty for the second term in Eq. (123). Whenever an $\hat{S} \in S$ exists which decreases the righthand side of Eq. (123), the solution to the LQG problem will necessarily generate such an $\hat{S}$, provided ϵ is sufficiently small.

If the function $\hat{S} - \hat{S}_o$ is "reasonably smooth," we may expect the two terms on the righthand side of Eq. (123) to be highly correlated so that each term must decrease individually, including $J_1(S)$ in particular; though no simple and precise conditions guaranteeing that $J_1(\hat{S})$ decreases seem possible.

To summarize we have, subject to seemingly reasonable assumptions, that $(\Delta\hat{Q}, \Delta\hat{R})$ cause $J_1(\hat{S})$ to decrease. So if the amount of decrease is uniformly bounded below by some continuous nonnegative strictly increasing function $\phi(J_1(\hat{S}))$, the problem of finding a feedback $\hat{F}(s)$ stablizing the plant $P(s)$ and satisfying Eq. (102) and (103) is in principle solvable via the following LQG-based iterative algorithm for reducing J_1 to its minimum:

Step 1: Choose any suitable initial values for $(\hat{Q}, \hat{\Xi}, \hat{R}, \hat{\theta})$.

Step 2: Solve the LQG problem for the $\hat{S} = \hat{S}_o$ and corresponding $\hat{F}$ which minimize $J_2(\hat{S})$. If Eq. (102) and (103) are satisfied, stop; otherwise continue.

Step 3: Leaving $(\hat{\Xi}, \hat{\theta})$ unchanged, choose some small $\epsilon > 0$ and modify $(\hat{Q}, \hat{R})$ according to the formula (112) - (115) and (121) and (122). Regurn to step 2.

(End of Algorithm)

This algorithm is of course highly idealized and has one especially noteworthy flaw: The functions $\Delta\hat{Q}$ and $\Delta\hat{R}_1$ given by Eq. (123) and (124) are irrational and consequently it is impractical to solve the LQG optimization problem exactly. In practice it will be necessary to approximate $\Delta\hat{Q}(-s^2)$ and $\Delta\hat{R}(-s^2)$ with rational functions of $-s^2$, possibly by approximating the irrational function $\delta_{-1}(\cdot)$ in Eq. (121) and (122) with functions of the form $\hat{\Phi}_* \hat{\Phi}$ where $\hat{\Phi}(s)$ is some, perhaps very coarse, rational approximation to a unity gain bandpass filter whose passbands coincide with the frequency ranges over which the term $\delta_{-1}(\cdot) \neq 0$. Since the complexity of the problem of solving the LQG optimization Eq. (110) at each iteration of the algorithm and the complexity of the resultant LQG feedback $\hat{F}(s)$ are in direct proportion to the number of poles in $(\hat{Q}, \hat{R}, \hat{\theta}, \hat{\Xi})$, we will in practice want to use a coarse approximation to $\Delta\hat{Q}$ and $\Delta\hat{R}$, having as few poles as possible. Whether or not a given approximation is too coarse and whether or not a given ϵ in Eq. (112) and (113) is sufficiently small may be readily checked at each iteration of the algorithm following minimization of J_2 by simply computing J_1 for $\hat{M}_1$ and $\hat{M}_2$ given by Eq. (119) and (120) and

checking to see if indeed J_1 is reduced by the $\hat{S}$ minimizing J_2. It is stressed that in design applications where the specifications (102) and (103) are fairly undemanding, it may often suffice to use extremely coarse approximations to $\Delta\hat{Q}$ and $\Delta\hat{R}$, possibly even constant approximations such as, for example, $\sup_{\omega} \Delta\hat{Q}(\omega^2)$ and $\sup_{\omega} \Delta\hat{R}(\omega^2)$, respectively. Since the quality of a given approximation is determined solely by whether $J_1(\hat{S})$ is reduced, it seems likely that the approximation to $(\Delta\hat{Q}, \Delta\hat{R})$ has to be most accurate at frequencies where $\Delta\hat{Q}$ or $\Delta\hat{R}_1$ are nonzero, while accuracy is relatively unimportant at frequencies where both $\Delta\hat{Q}$ and $\Delta\hat{R}_1$ are zero.

Note that the LQG optimization of Eq. (110) and (111) is completely symmetric with respect to the roles played by $(\hat{Q}, \hat{R})$ and $(\hat{\Xi}, \hat{\theta})$. Consequently, we may exchange $(\hat{Q}, \hat{R})$ with $(\hat{\Xi}, \hat{\theta})$ in Eq. (112)-(122) and thereby obtain a "dual" procedure for synthesis of a stabilizing feedback satisfying Eq. (102) and (103) in which $(\hat{Q}, \hat{R})$ are held fixed and $\hat{\Xi}$ and $\hat{\theta}$ are varied at each iteration of the design algorithm.

Insofar as satisfying closed-loop system design specifications on noise response, tracking error, sensitivity, and stability margins is concerned, there is no reason to prefer varying $(\hat{Q}, \hat{R})$ over varying $(\hat{\Xi}, \hat{\theta})$ or vice versa: both procedures will tend to lead to a design that meets the specifications of Eq. (102) and (103).

As a final remark, we note that closed-loop system poles are precisely the left-half plane zeros of

$$\hat{R} + \hat{P}_* \hat{Q} \hat{P}$$

and

$$\hat{\theta} + \hat{P}\hat{\Xi}\hat{P}_{*} \tag{124}$$

so closed-loop poles are directly related to the choice of $(\hat{Q}, \hat{R}, \hat{\Xi}, \hat{\theta})$. However, because an LQG optimal feedback design can have a fairly complicated closed-loop transfer function $\hat{T}(s)$, classical root locus design intuition based on the behavior of a system with one or two dominant poles and no nearby zeros may be of little value. That is, closed-loop pole location by themselves may not always provide readily interpretable information about a system's transient response. We note that the complexity of a system's closed-loop transfer function has no bearing on the interpretation of frequency response quantities such as $|\hat{S}|^2$ and $|\hat{T}|^2$ (which are directly related to system sensitivity, RMS noise response, RMS tracking errors, and stability margins).

The Multivariable Case

We now consider the multivariable analog of the ideas developed in the preceeding subsection. The problem is to design a stabilizing MIMO proper rational feedback $\hat{F}(s)$ for a MIMO strictly proper rational $\hat{P}(s)$ to stabilize the closed-loop system

$$\hat{y}(s) = \hat{P}(s)\,\hat{u}(s) \tag{125}$$

$$\hat{u}(s) = \hat{F}(s) \cdot (\hat{r}(s) - \hat{y}(s)) \tag{126}$$

and satisfy the contraints

$$\sigma_{max}(\hat{Q}_s^{\frac{1}{2}}(r) \cdot \hat{S} \cdot \hat{\Xi}_s^{\frac{1}{2}}(\ell)) < 1 \quad \forall\omega \tag{127}$$

$$\sigma_{max}(\hat{R}_s^{\frac{1}{2}}(r) \cdot \hat{T} \cdot \hat{\theta}_s^{\frac{1}{2}}(\ell)) < 1 \quad \forall\omega \tag{128}$$

where

$(\hat{Q}_s,\ \hat{\Xi}_s,\ \hat{R}_s,\ \hat{\theta}_s)$ are para-hermitian rational functions of $-s^2$ which are uniformly bounded and uniformly positive definite on the $j\omega$-axis with

$$\lim_{\omega \to \infty} \sigma_{max}\left(\hat{Q}_s^{\frac{1}{2}}(r)\ \ \hat{\Xi}_s^{\frac{1}{2}}(\ell)\right) < 1 \text{ and where}$$

$$\hat{S} \triangleq I - \hat{T} \triangleq (I + \hat{P}\hat{F})^{-1} \tag{129}$$

The variables $(\hat{Q}_s,\ \hat{\Xi}_s,\ \hat{R}_s,\ \hat{\theta}_s)$ play a role analogous to ρ_1 and ρ_2 in Eq. (101)-(103) and may be selected to reflect design specifications on sensitivities, stability margin, noise response, tracking error, and so forth. We assume that $p \triangleq \dim(y) = \dim(u)$, that is, there are exactly as many sensors as there are actuators and that

$$\det(\hat{P}(s)) \not\equiv 0^{\dagger} \tag{130}$$

When a solution to the foregoing feedback synthesis problem exists the problem is equivalent to solving the optimization problem

$$\min_{\hat{S} \in S} \quad J_1(\hat{S}) \tag{131}$$

---

†This condition should be distinguished from the more restrictive condition $\det(\hat{P}) \not\equiv 0\ \forall\ s$, which would imply that $\hat{P}$ has no transmission zeros. This condition (Eq. 130) is, loosely speaking, equivalent to requiring that each sensor measure something different.

where

$$J_1(\hat{S}) \triangleq \frac{1}{2\pi} \int_{-\infty}^{\infty} \mathrm{Tr}(\hat{W}_1 \cdot \hat{S} \cdot \hat{M}_1 \cdot \hat{S}_* + \hat{W}_2 \cdot (I - \hat{S}) \cdot \hat{M}_2 (I - \hat{S})_*)\, d\omega \tag{132}$$

$$S \triangleq \left\{ \hat{S} \mid \hat{S} = (I + PF)^{-1};\ \hat{F} \text{ proper and rational; the closed-loop system of Eq. (100) and (101) has no poles in } \mathrm{Re}(s) \geq 0 \right\} \tag{133}$$

$$W_1(\hat{S}) \triangleq \sum_{r=1}^{p} \left\{ \left(\hat{Q}_s^{\frac{1}{2}}(r) \right)_* \cdot \hat{u}_i \hat{u}_i^* \cdot \hat{Q}_s^{\frac{1}{2}}(r) \cdot \delta_{-1}\left(\sigma_i \left(\hat{Q}_s^{\frac{1}{2}}(r)\, \hat{S}\, \hat{\Xi}_s^{\frac{1}{2}}(\ell) \right) - 1 \right) \right\} \tag{134a}$$

$$\hat{W}_2(\hat{T}) \triangleq \sum_{i=i}^{p} \left\{ \left(\hat{R}_s^{\frac{1}{2}}(r) \right)_I \cdot \hat{v}_i \hat{v}_{i*} \cdot \hat{R}_s^{\frac{1}{2}}(r) \cdot \delta_{-1}\left(\sigma_i \left(\hat{R}_s^{\frac{1}{2}}(r) \cdot \hat{T} \cdot \hat{\theta}_s^{\frac{1}{2}}(\ell) \right) - 1 \right) \right. \tag{134b}$$

u_i is the ith left singular vector of

$$\hat{Q}_s^{\frac{1}{2}}(r) \cdot \hat{S} \cdot \hat{\Xi}_s^{\frac{1}{2}}(\ell)$$

v_i is the i_{th} left singular vector of

$$\hat{R}_s^{\frac{1}{2}}(r) \cdot \hat{T} \cdot \hat{\theta}_s^{\frac{1}{2}}(\ell)$$

and $\hat{M}_1$ and $\hat{M}_2$ are positive definite on the jω axis but otherwise arbitrary.

Note that $J_1(\hat{S}) > 0$ unless Eq. (127)-(130) are satisfied, in which case $J_1(\hat{S}) = 0$. In order to ensure that J_1 has no local minima at which $J_1(\hat{S}) > 0$ (at least when an S_o satisfying Eq. (127) and (128) exists) we choose

$$\hat{M}_1 = \hat{\alpha}_1 \cdot \hat{\Xi}_s \tag{135a}$$

$$\hat{M}_2 = \hat{\alpha}_2 \cdot \hat{\theta}_s \tag{135b}$$

(see Lemma D, Appendix G) where $\hat{\alpha}_1$ and $\hat{\alpha}_2$ are any specified scalar functions of $-s^2$ that are real-valued and positive along the $j\omega$-axis. Thus, provided an $\hat{S} \in S$ satisfying Eq. (127) and (128) exists, then in every neighborhood of each $\hat{S}_1$ at which $J_1(\hat{S}_1) > 0$, there is an $\hat{S}_2$ with

$$J_1(\hat{S}_2) < J_1(\hat{S}_1)$$

As in the SISO case, LQG stochastic optimal control theory provides a systematic method for generating such an $\hat{S}_2$.

The LQG theory provides a method for solving the stochastic linear optimal control problem

$$\min_{\hat{S} \in S} \left(\frac{1}{2\pi}\right) \int_{-\infty}^{\infty} [\hat{Y}_* \hat{Q} \hat{Y} + \hat{u}_* \hat{R} \hat{u}] \, d\omega \tag{136}$$

subject to

$$\hat{Y} = \hat{P} (\hat{u} + \hat{\xi}) \tag{137}$$

$$\hat{u} = -\hat{F} (\hat{Y} + \hat{\theta}) \tag{138}$$

where $(\hat{\xi}, \hat{\theta})$ are zero mean stochastic noise with respective power spectra $(\hat{\Xi}, \hat{\theta})$

Note that $(\hat{Q}(-s^2),\ \hat{\Xi}(-s^2),\ \hat{R}(-s^2),\ \theta\text{-}s^2))$ are distinct from the $(\hat{Q}_s,\ \hat{R}_s,\ \hat{\Xi}_s,\ \vartheta_s)$ in Eq. (127) and (128). The LQG optimization of Eq. (136)-(138) may be solved by matrix spectral factorization[27] or (with the aid of an augmented plant model to incorporate the s^2-dependence of $(\hat{Q},\ \hat{\Xi},\ \hat{R},\ \hat{\theta})$) by the solution of the algebraic Riccati equations. With a few computations, it can be shown that the LQG optimization is equivalent to the unconstrained optimization problem.

$$\min_{\hat{S} \in S} \quad J_2(S) \tag{139}$$

where

$$\begin{aligned} J_2(\hat{S}) = \frac{1}{2\pi} \int_{-\infty}^{\infty} \Big\{ & \mathrm{Tr}\,(\hat{Q}\ \hat{S}\ \hat{P}\ \hat{\Xi}\ \hat{P}_*\ \hat{S}_*) \\ & + \mathrm{TR}\Big(\hat{Q}\ (I - \hat{S})\ \hat{\theta}\ (I - \hat{S})_* \\ & + P_*^{-1}\ \hat{R}\ P^{-1}\ (I - \hat{S})\ \hat{P}\ \hat{\Xi}\ \hat{P}_*\ (I - \hat{S})_* \\ & + \hat{P}_*^{-1}\ \hat{R}\ \hat{P}^{-1}\ (I - \hat{S})\ \hat{\theta}\ (I - \hat{S})_* \Big) \Big\}\ d\omega \end{aligned} \tag{140}$$

The connection between the LQG optimization and Eq. (131) can be seen by examining the effect of certain small perturbations $(\Delta\hat{Q},\ \Delta\hat{R})$ on the value of $J_2(\hat{S})$

$$\hat{Q} \leftarrow \hat{Q} + \epsilon\Delta\hat{Q} \tag{141}$$

$$\hat{R} \leftarrow \hat{R} + \epsilon\Delta\hat{R} \tag{142}$$

where

$$\Delta\hat{R} = \Delta\hat{R}_1 + \Delta\hat{R}_2 \tag{143}$$

$$\Delta\hat{R}_2 = -P_* \hat{T}_{o*} - 1 \left[\left(\hat{\theta} + \hat{P} \hat{\Xi} \hat{P}_* \right)^{\frac{1}{2}(\ell)} \right]_*^{-1}$$

$$\cdot \left[\hat{\theta}_*^{\frac{1}{2}(\ell)} \hat{T}_{0*} \Delta\hat{Q} \hat{T}_o \hat{\theta}^{\frac{1}{2}(\ell)} \right.$$

$$\left. + \hat{\Xi}_*^{\frac{1}{2}(\ell)} \cdot \hat{P}_* \cdot \hat{T}_{o*} \cdot \hat{P}_*^{-1} \cdot \Delta\hat{R}_1 \cdot \hat{P}^{-1} \cdot \hat{T}_o \cdot \hat{P} \cdot \hat{\Xi}^{\frac{1}{2}(\ell)} \right]$$

$$\left[\left(\hat{\theta} + \hat{P} \hat{\Xi} \hat{P}_* \right)^{\frac{1}{2}(\ell)} \right]^{-1} \cdot \hat{T}_o^{-1} \hat{P} \tag{144}$$

With this perturbation to $(\hat{Q}, \hat{R})$, the resulting perturbation to J_2 is for any <u>fixed</u> $\hat{S} \triangleq I - \hat{T}$ given by

$$\Delta J_2(\hat{S}) = \epsilon \frac{1}{2\pi} \int_{-\infty}^{\infty} \left[\mathrm{Tr} \left(\Delta\hat{Q} \hat{S} \hat{P} \hat{\Xi} \hat{P}_* \hat{S}_* \right) \right.$$

$$\left. + \mathrm{Tr} \left(\hat{P}_*^{-1} \Delta\hat{R}_1 \hat{P}^{-1} (I - \hat{S}) \hat{\theta} (I - \hat{S}) \right) \right] d\omega \tag{145}$$

If we choose

$$\Delta\hat{Q} = \hat{W}_1 (\hat{S}_o) \tag{146}$$

$$\Delta\hat{R}_1 = \hat{R}_* \cdot \hat{W}_2 (I - \hat{S}_o) \cdot \hat{P} \tag{147}$$

and take $\hat{\Xi}$ and $\hat{\theta}$ such that

$$\hat{M}_1 = \hat{P} \hat{\Xi} \hat{P}_* = \hat{\alpha}_1 \cdot \hat{\Xi}_s \tag{148}$$

$$\hat{M}_2 = \hat{\theta} = \hat{\alpha}_2 \cdot \hat{\theta}_s \tag{149}$$

for some real-valued uniformly positive, uniformly-bounded ω^2 dependent scalars $\hat{\alpha}_1$ and $\hat{\alpha}_2$, then

$$\Delta J_2(\hat{S}) = \epsilon J_1(\hat{S}) + \frac{\epsilon}{2\pi} \int_{-\infty}^{\infty} \Big\{ \mathrm{Tr} \quad (\hat{W}_1(\hat{S}_o) - \hat{W}_1(\hat{S})) \cdot \hat{S} \hat{M}_1 \hat{S}_*$$

$$+ (\hat{W}_2 (I - \hat{S}_o) - \hat{W}_2 (I - \hat{S}) (I - \hat{S}) \hat{M}_2 (I - \hat{S})_* \Big\} d\omega \tag{150}$$

We conclude that provided $(\hat{M}_1, \hat{M}_2, \hat{\Xi}, \hat{\theta})$ satisfy Eq. (148) and (149), then the perturbations $(\Delta\hat{Q}, \Delta\hat{R})$ given by Eq. (141)-(144) and Eq. (146) and (147) tend for ϵ sufficiently small to perturb the minimizing values of $\hat{S}$ for the LQG problem of Eq. (140) in such a way as to reduce $J_1(\hat{S})$ whenever $J_1(\hat{S}) > 0$ and an $\hat{S} \in S$ exists satisfying Eq. (127) and (128).

Thus, the cost weighting matrix perturbations $(\Delta\hat{Q}, \Delta\hat{R})$ given by Eq. (141)-(144) and Eq. (145) and (146) tend to generate an LQG optimal feedback that satisfies the constraints of Eq. (127) and (128) and stabilizes the plant $\hat{P}(s)$. As in the SISO case, the $\Delta\hat{Q}$ and $\Delta\hat{R}$ are in general irrational and must be approximated at each iteration by rational matrixes. Accuracy of the approximation is the most important at frequencies and in "singular-vector directions" where $(\Delta\hat{Q}, \Delta\hat{R}_1)$ are nonzero.

Conclusion

As a method for meeting frequency-response inequality specifications on closed-loop system robustness, the LQG theory has been examined. An algorithm for iterative adjustment of the frequency-dependent noise/cost matrixes ($\hat{Q}$, $\hat{\Xi}$, R, $\hat{\theta}$) has been described which, under reasonable but as yet imprecisely formulated assumptions, is globally convergent to a feedback design meeting the specifications. However, because exact implementation of the algorithm requires solution of infinite dimensional LQG problems (infinite dimensional Riccati equations or spectral factorization of irrational transfer functions), the algorithm can be only approximately implemented in practice. When suitable approximations are employed, the algorithm appears to provide a viable engineering methodology for the synthesis of robust multivariable feedback control systems.

REFERENCES

1. Hartmann, G.L. Harvey, C.A., and Mueller, C.E., "Optical Linear Control (Formulation to Meet Conventional Design Specs.)," ONR CR215-238-1, Honeywell Systems and Research Center, Minneapolis, Minnesota, March 1976.

2. Doyle, J.C., "Guaranteed Margins for LQG Regulators," IEEE Trans. Automat. Contr., Vol. AC-23, No. 4, August 1978, pp. 756-757.

3. Harvey, C.A., and Doyle, J.C., "Optimal Linear Control (Characterization and Loop Transmission Properties of Multivariable Systems)," ONR Report No. CR215-238-3, Honeywell Systems and Research Center, Minneapolis, Minnesota, August 1978.

4. Doyle, J.C. and Stein, G., "Robustness with Observers," IEEE Trans. Automat. Contr., Vol. AC-24, No. 4, August 1979, pp. 607-611.

5. Harvey, C.A., Stein, G., and Doyle, J.C., "Optimal Linear Control (Characterization of Multi-Input Systems)," ONR CR215-238-2, Honeywell Systems and Research Center, Minneapolis, Minnesota, August 1977.

6. Harvey, C.A., and Stein, G., "Quadratic Weights for Asymptotic Regulator Properties," IEEE Trans. Automat. Contr., Vol. AC-23, No. 3, June 1978, pp. 378-387.

7. Stein, G. "Generalized Quadratic Weights for Asymptotic Regulator Properties," IEEE Trans. Automat. Contr., Vol. AC-24, No. 4, August 1979, pp. 559-566.

8. Harvey, C.A., and Stein, G., "Linear Multivariable Control Design Based on Asymptotic Regulator Properties," in Alternatives for Linear Multivariable Control, National Engineering Consortium, Inc., Chicago, 1978, pp. 355-367.

REFERENCES (continued)

9. Horowitz, I. M., Synthesis of Feedback Systems. New York: Academic Press, 1963.

10. Background Information and User Guide for MIL-F-94900, Report AFFDL-TR-24-116, Air Force Flight Dynamics Laboratory, January 1975.

11. Rosenbrock, H. H., Computer-Aided Control System Design. New York: Academic Press, 1974.

12. MacFarlane, A. G. J., and Kouvaritakis, B., "A Design Technique for Linear Multivariable Feedback Systems," International Journal of Control, Vol. 23, No. 6, June 1977, pp. 837-874.

13. Doyle, J. C., "Robustness of Multivariable Linear Feedback Systems," Proc. IEEE Conf. on Decision and Control, San Diego, California, January 10-12, 1979.

14. Sandell, N. R., "Singular Values and Robustness," Proc. Allerton Conference on Communication, Control, and Computing, Monticello, Illinois, October 1978.

15. Safonov, M. G., "Robustness and Stability Aspects of Stochastic Multivariable Feedback Design," PhD Dissertation, MIT, September 1977.

16. Safonov, M. G., "Tight Bounds on the Response of Multivariable Systems with Component Uncertainty," Proc. Allerton Conference on Communication, Control, and Computing, Monticello, Illinois, October 1978.

17. Laub, A. J., "Computational Aspects of Singular Value Decomposition," Proc. Allerton Conference on Communication, Control, and Computing, Monticello, Illinois, October 1978.

18. Ostroff, A. J., Downing, D. R., and Road, W. J., "A Technique Using a Nonlinear Helicopter Model for Determining Terms and Derivations," NASA Technical Note TN D-8159, NASA-Langley Research Center, May 1976.

REFERENCES (concluded)

19. Hohenemser, R.H., and Yin, S., "Some Application of the Method of Multiblade Coordinates," Journal of American Helicopter Society, July 1972.

20. Stein, G., "Generalized Quadratic Weights for Asymptotic Regulator Properties," IEEE Trans. Auto. Control, Vol. AC-24, No. 4, August 1979, pp. 559-566.

21. Kalman, R.E., "When is a Linear System Optimal?" Journal of Basic Engineering, Vol. 86, 1964, pp. 51-60.

22. Youla, D.C., "On the Factorization of Rational Transfer Function Matrices," IRE Trans. on Information Theory, July, 1961. pp. 172-182.

23. Safonov, M.G., and Athans, M., "A Multiloop Generalization of the Circle Stability Criterion," Proc. Asilomar Conference on Circuits, Systems and Computers, Pacific Grove, California, November 6-8, 1978.

24. Athans, M., "The Role and Use of the Stochastic Linear-Quadratic-Gaussian Problem in Control System Design," IEEE Trans. on Automatic Control, Vol. AC-16, 1971, pp. 529-552.

25. Youla, D.C., et al., "Modern Wiener-Hopf Design of Optimal Controllers Part I: The Single-Input-Output Case," IEEE Trans. on Automatic Control, Vol. AC-21, 1976, pp. 3-13.

26. Youla, D.C., et al., "Modern Wiener-Hopf Design of Optimal Controllers--Part II: The Multivariable Case," IEEE Trans. On Automatic Control, Vol. AC-21, 1976, pp. 319-338.

27. Shaked, U., "A General Transfer Function Approach to the Steady-State Linear Quadratic Gaussian Stochastic Control Problem," International Journal of Control, Vol. 24, 1976, pp. 771-800.

APPENDIX A

LEMMA A (FREQUENCY-DOMAIN CONICITY TEST)

Let P(s) and Q(s) be proper rational para-hermitian matrixes of full normal rank; P(s) is uniformly positive definite on the $s = j\omega$ axis and Q(s) is positive definite on the $s = j\omega$ axis. Let C(s) be a proper rational matrix which has no poles in $\mathrm{Re}(s) \geq 0$. Let $\underset{\sim}{T}$ be a stable operator. If for some $\epsilon > 0$ and every input-output pair $(\underline{u}, \underline{y})$ satisfying $\underline{y} = \underset{\sim}{T}\,\underline{u}$ we have

$$\int_{-\infty}^{\infty} \left|\left| \underline{Q}^{\frac{1}{2}}(j\omega) \left(\underline{Y}(j\omega) - \underline{C}(j\omega)\,\underline{U}(j\omega) \right) \right|\right|^2 d\omega$$

$$\leq \int_{-\infty}^{\infty} \left(\left|\left| \underline{P}^{\frac{1}{2}}(j\omega)\,\underline{U}(j\omega) \right|\right|^2 - \epsilon \left|\left| \underline{U}(j\omega) \right|\right|^2 \right) d\omega \qquad \text{(A-1)}$$

Then

$$\underset{\sim}{T} \ \underline{\text{inside}}\ L_{2e}\text{-Cone}\ (\underset{\sim}{C},\ \underset{\sim}{P}^{\frac{1}{2}},\ \underset{\sim}{Q}^{\frac{1}{2}}) \qquad \text{(A-2)}$$

where $\underset{\sim}{C}$, $\underset{\sim}{P}^{\frac{1}{2}}$, $\underset{\sim}{Q}^{\frac{1}{2}}$ are the LTI operator whose impulse responses are the inverse Fourier transforms of $C(j\omega)$, $P^{\frac{1}{2}}(j\omega)$, $Q^{\frac{1}{2}}(j\omega)$. If additionally Eq. (58) holds for some $\epsilon > 0$, then

$$\underset{\sim}{T} \ \underline{\text{strictly inside}}\ L_{2e}\text{-Cone}\ (\underset{\sim}{T},\ \underset{\sim}{P}^{\frac{1}{2}},\ \underset{\sim}{Q}^{\frac{1}{2}}) \qquad \text{(A-3)}$$

If the assumption that C(s) has no poles in $R(s) \geq 0$ is relaxed to no poles on the $j\omega$-axis then Eq. (A-2) and (A-3) hold if one substitutes "L_2-Cone $(\underset{\sim}{C}, \underset{\sim}{P}^{\frac{1}{2}}, \underset{\sim}{Q}^{\frac{1}{2}})$" for "$L_{2e}$ - Cone $(\underset{\sim}{C}, \underset{\sim}{P}^{\frac{1}{2}}, \underset{\sim}{Q}^{\frac{1}{2}})$."

PROOF OF LEMMA A:

We first consider the more difficult L_{2e}-Cone case. Let $\underset{\sim}{P}^{\frac{1}{2}}$ denote the nonanticipative minimum phase LTI operator whose impulse response is the inverse Fourier transform of $P^{\frac{1}{2}}(j\omega)$. Let ω_τ and y satisfy

$$w_\tau(t) = \begin{cases} (\underset{\sim}{P}^{\frac{1}{2}} u)(t), & \text{if } t \leq \tau \\ 0 & \text{if } t > \tau \end{cases}$$

$$\underline{y} = \underset{\sim}{T}\,\underline{u}$$

Let $Y(j\omega)$ and $W_\tau(j\omega)$ denote the respective Fourier transforms of $\underline{y}_\tau$ and $\underline{w}_\tau$. Then

$$\begin{aligned} \|\underset{\sim}{Q}^{\frac{1}{2}}(\underline{y} - \underset{\sim}{C}\,\underline{u})\|_\tau^2 &= \|\underset{\sim}{Q}^{\frac{1}{2}}(\underline{y} - \underset{\sim}{C}\,\underset{\sim}{P}^{-\frac{1}{2}}\,\underset{\sim}{P}^{\frac{1}{2}}\,\underline{u})\|_\tau \\ &= \|\underset{\sim}{Q}^{\frac{1}{2}}(\underline{y} - \underset{\sim}{C}\,\underset{\sim}{P}^{-\frac{1}{2}}\,\underline{w}_\tau)\|_\tau^2 \\ &\quad \text{(By causality of } \underset{\sim}{P}^{\frac{1}{2}}\,\underset{\sim}{C}\,\underset{\sim}{R}^{-\frac{1}{2}}) \\ &\leq \int_{-\infty}^{\infty} \|Q^{\frac{1}{2}}(y - \underset{\sim}{C}\,\underset{\sim}{P}^{-\frac{1}{2}}\,\underline{w}_\tau\|^2 \quad dt \\ &= \int_{-\infty}^{\infty} \|\underline{Q}^{\frac{1}{2}}(j\omega)\,(\underline{Y}(j\omega) - \underline{C}(j\omega)\,P^{-\frac{1}{2}}(j\omega)\,\underline{W}_\tau(j\omega)\|^2 \\ &\quad d\omega \end{aligned}$$

(by Parseval's Theorem)

$$= \int_{-\infty}^{\infty} ||W_\tau(jw)||^2 - \epsilon \int_{-\infty}^{\infty} ||P^{-\frac{1}{2}}(jw)\, W_\tau||^2 \quad dw$$

(by Eq. (A-1))

$$= ||\underline{W}_\tau||_{L_2}^2 - \epsilon\, ||\underset{\sim}{P}^{-\frac{1}{2}}\, W_{-\tau}||_{L_2}$$

(By Parseval's Theorem)

$$\leq ||W_\tau||_\tau^2 - \epsilon\, ||P^{-\frac{1}{2}} W_\tau||_\tau$$

(Since $W_\tau(t) = 0$ if $t \geq \tau$, and $||\underline{z}||_{L_2} \geq ||z||_\tau \; \forall \; \underline{z}$.)

$$= ||\underset{\sim}{P}^{\frac{1}{2}} \underline{u}||_\tau^2 - \epsilon\, ||u||_\tau^2$$

(Since for $t \leq \tau$ $P^{\frac{1}{2}} \underline{u}(t) = W_\tau(t)$ and $\underset{\sim}{P}^{-\frac{1}{2}}\, \underset{\sim}{P}^{\frac{1}{2}} = \underset{\sim}{I}$.)

$$\leq ||\underset{\sim}{P}^{\frac{1}{2}} \underline{u}||_\tau^2 - \epsilon' ||\underline{u}||_\tau^2$$

where

$$\epsilon' = \epsilon \; \frac{1}{1+g}$$

$$g = \sup \; \frac{||\underset{\sim}{T}\, u||_\tau}{\tau\, ||u||_\tau}$$

The L_2-Cone case in which C(s) is permitted to have poles in $(R(s)) > 0$ but no poles on the $s=j\omega$ axis follows trivially from Parseval's Theorem.

(End of Proof)

APPENDIX B

LEMMA B

FREQUENCY-DOMAIN TEST FOR "OUTSIDE" L_{2e}-CONICITY OF INVERSE RELATIONS

Let P(s) and Q(s) be proper rational para-hermitian transfer function matrixes of full normal rank;[1] suppose P(s) is positive definite on the $s = j\omega$ axis and Q(s) is uniformly positive definite on the $s = j\omega$ axis. Let $\underset{\sim}{G}$, $\underset{\sim}{C}$ be LTI operators with transform functions G(s), C(s) and suppose that the LTI system

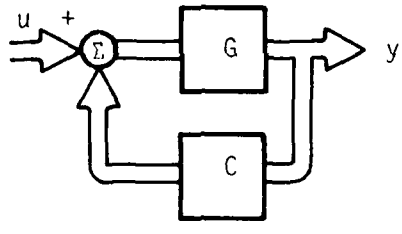

is stable and nonanticipative.

If for all

$$Q(j\omega) - \left[G(j\omega)\,(I + C(j\omega)\,G(j\omega)\right]^{*}\; P(j\omega)\; \left[G(j\omega)\,(I + CG(j\omega)\right]^{-1} \qquad \text{(B-1)}$$

is positive semidefinite, then $\underset{\sim}{G}^{I}$ (the inverse relation of G) satisfies

---

[1] D. C. Youla, "On the Factorization of Rational Transfer Function Matrices," IRE Trans. on Information Theory, July, 1961. pp. 172-182.

$\underset{\sim}{G}^{I}$ outside L_{2e}-Cone ($\underset{\sim}{C}$, $\underset{\sim}{P}^{\frac{1}{2}}$, $\underset{\sim}{Q}^{\frac{1}{2}}$)

PROOF OF LEMMA B

Let (x, y) be any input-output pair satisfying

$$y = \underset{\sim}{G}x \tag{B-2}$$

Let

$$v = \underset{\sim}{Q}^{\frac{1}{2}}(x - \underset{\sim}{C}y) \tag{B-3}$$

and

$$V_\tau = \begin{cases} V(t), & \text{if } t \leq \tau \\ 0, & \text{if } t > \tau \end{cases} \tag{B-4}$$

This relation is established by the system

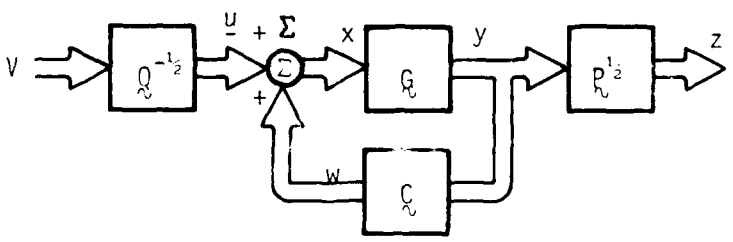

(which by hypothesis is a stable system).

Let $V(j\omega)$ denote the Fourier transform of $V_\tau(j\omega)$. Note that from (B-1), it follows that for every complex $V_\tau(j\omega)$

AD-A083 130 HONEYWELL SYSTEMS AND RESEARCH CENTER MINNEAPOLIS MN F/G 12/1
OPTIMAL LINEAR CONTROL.(U)
DEC 79 C A HARVEY, M G SAFONOV, G STEIN N00014-75-C-0144
UNCLASSIFIED 79SRC87 ONR-CR215-238-4F NL

2 of 2
AD
A083130

END
DATE FILMED
5-80
DTIC

$$||V_\tau(j\omega)||^2 - ||P^{\frac{1}{2}}(j\omega)\, G(j\omega)\, (I + C(j\omega)\, G(j\omega))^{-1}\, Q^{-\frac{1}{2}}(j\omega)\, V_\tau(j\omega)||^2$$

$$= \left[Q^{-\frac{1}{2}}(j\omega)\, V_\tau(j\omega)\right]^* \left[Q(j\omega) - \left(P^{\frac{1}{2}}(j\omega)\, G(j\omega)\right.\right.$$

$$\bullet \quad \left.\left(I + C(j\omega)\, G(j\omega)\right)^{-1} Q^{-\frac{1}{2}}(j\omega)\right)^* P(j\omega)$$

$$\bullet \quad (P^{\frac{1}{2}}(j\omega)\, G(j\omega)\, (I + C(j\omega)\, G(j\omega))^{-1}\, Q^{-\frac{1}{2}}(j\omega)\Big] \qquad \text{(B-5)}$$

$$\bullet \quad \left[Q^{-\frac{1}{2}}(j\omega)\, V_\tau(j\omega)\right] \geq 0$$

Now for x, y, v, and v defined as above we have

$$||\underset{\sim}{P}^{\frac{1}{2}} y||_\tau^2 = ||\underset{\sim}{P}^{\frac{1}{2}} \underset{\sim}{G}\, (\underset{\sim}{I} + \underset{\sim}{C}\underset{\sim}{G})^{-1}\, \underset{\sim}{Q}^{-\frac{1}{2}}\, v||_\tau^2$$

$$= ||\underset{\sim}{P}^{\frac{1}{2}}\, \underset{\sim}{G}\, (I + CG)^{-1}\, Q^{-\frac{1}{2}}\, v_\tau||_\tau^2$$

(by causality of $\underset{\sim}{P}^{\frac{1}{2}} \underset{\sim}{G}(\underset{\sim}{I} + \underset{\sim}{C}\underset{\sim}{G})^{-1}\, \underset{\sim}{Q}^{-\frac{1}{2}}$)

$$\leq \int_0^\infty ||(\underset{\sim}{P}^{\frac{1}{2}} \underset{\sim}{G}(\underset{\sim}{I} + \underset{\sim}{C}\underset{\sim}{G})^{-1}\, \underset{\sim}{Q}^{-\frac{1}{2}}\, v_\tau)(t)||^2\, dt$$

(This integral exists since $\underset{\sim}{P}^{\frac{1}{2}} \underset{\sim}{G}(\underset{\sim}{I} + \underset{\sim}{C}\underset{\sim}{G})^{-1}\, \underset{\sim}{Q}^{-\frac{1}{2}}$ is stable.)

$$= \int_{-\infty}^\infty ||P^{\frac{1}{2}}(j\omega)\, G(j\omega) \left(I + C(j\omega)\, G(j\omega)\right)^{-1} Q^{-\frac{1}{2}}(j\omega)\, V_\tau(j\omega)||^2\, d\omega$$

(By Parseval's theorem and the stability of $\underset{\sim}{P}^{\frac{1}{2}} \underset{\sim}{G}(\underset{\sim}{I} + \underset{\sim}{C}\underset{\sim}{G})\, \underset{\sim}{Q}^{-\frac{1}{2}}$.)

$$\leq \int_{-\infty}^\infty ||V_\tau(j\omega)||^2\, d\omega$$

(By condition (B-5).)

$$= \int_0^{\infty} \|V_\tau(t)\|^2 \, dt$$

(By Parseval's theorem)

$$= \int_0^{\tau} \|V_\tau(t)\|^2 \, dt$$

Since $V_\tau(t) = 0$, if $t > \tau$

$$= \int_0^{\tau} \|v(t)\|^2 \, dt$$

$$\triangleq \|v\|_\tau^2 = \|\underset{\sim}{Q}^{\frac{1}{2}} u\|_\tau^2$$

$$= \|\underset{\sim}{Q}^{\frac{1}{2}} (x - \underset{\sim}{C} y)\|_\tau^2$$

Thus,

G^I outside Cone $(\underset{\sim}{C}, \underset{\sim}{P}^{\frac{1}{2}}, \underset{\sim}{Q}^{\frac{1}{2}})$

(End of Proof)

APPENDIX C

LEMMA C

If $Q \in C^{nxn}$ is a hermitian positive definite matrix, and $B \in C^{rxn}$ is a matrix of full rank $r \leq n$, then the matrix $\tilde{Q} = (B\,Q^{-1}\,B^{*})^{-1}$ has the properties that

a. $Q - B^{*}\tilde{Q}B \geq 0$

b. if S is any other matrix such that $Q - B^{*}SB \geq 0$ then $\tilde{Q} \geq S$

PROOF OF LEMMA C

Consider the C^{n} spaces $C_Q^{\,n}$ with inner product $\langle x_1, x_2 \rangle_Q = x_1^{*}Qx_2$ and $C_I^{\,r}$ with inner product $\langle y_1, y_2 \rangle_I = y_1^{*}y_2$. Consider the matrix B as a linear mapping of $C_Q^{\,n}$ into $C_I^{\,r}$. Then, if we denote the adjoint mapping of B as B^{a}, we have

$$x_1^{*}Bx_2 \triangleq \langle x_1, Bx_2 \rangle_I$$

$$= \langle B^{a}x_1, x_2 \rangle_Q$$

$$= x_1^{*}(B^{a})^{*}Qx_2 \qquad \text{(C-1)}$$

For all $x_1, x_2 \in C_Q^n$. Hence

$$B = \left(B^a\right)^* \tag{C-2}$$

$$\left(B^a\right)^* = B\,Q^{-1} \tag{C-3}$$

Thus, the pseudo-inverse (or, Moore-Penrose inverse) of B is

$$\begin{aligned} B^\dagger &= B^a \left[BB^a\right]^{-1} \\ &= Q^{-1} B^* \left[B\,Q^{-1} B^*\right]^{-1} \end{aligned} \tag{C-4}$$

Thus,

$$\begin{aligned} \tilde{Q} &\triangleq (B\,Q^{-1} B^*)^{-1} = (B\,Q^{-1} B^*)^{-1} B\,Q^{-1} Q\,Q^{-1} B^* (B\,Q^{-1} B^*)^{-1} \\ &= (B^\dagger)^* Q\,B^\dagger \end{aligned} \tag{C-5}$$

Now, let $x_1 + x_2$ be the orthogonal decomposition of a vector $x \in C_Q^n$

$$x = x_1 + x_2 \tag{C-6}$$

where

x_1 = projection of x onto the null space of B

x_2 = projection of x onto the orthogonal complement of the null space of B (so, $\langle x_2, x_1 \rangle_Q = 0$)

The matrix $B^\dagger$ has this property that for all x

$$B^\dagger B\, x = Bx_2 \tag{C-7}$$

Thus,

$$x^*(Q - B^* \tilde{Q} B)\, x$$

$$= (x_1 + x_2)^*(Q - (B^\dagger B)^* Q(B^\dagger B))\, x_1 + x_2$$

$$= x_1^*\, Q\, x_1 + x_2^*\, Q\, x_1 + x_1^* Q\, x_2 + x_2^*\, Q x_2$$

$$-x_2^*\, Q\, x_2$$

(Since $B^\dagger B\, x_1 = 0$) (C-8)

$$= \langle x_1, x_1 \rangle_Q + \langle x_2, x_1 \rangle_Q + \langle x_2, x_1 \rangle_Q$$

$$= \langle x_1, x_1 \rangle_Q \tag{C-9}$$

$$\geq 0$$

which establishes claim a.

Let S be any matrix satisfying

$$Q - B^* S B \geq 0 \tag{C-10}$$

Then, since $BB^\dagger = I$, we have for any $y \in C_I^r$, that $B^\dagger y = x_2$ is in the orthogonal complement of the null space of B and hence

$$y^* S y = y^*(B^\dagger)^* B^* S B B^\dagger y \tag{C-11}$$

$$= x_2^* B^* S B x_2 \tag{C-12}$$

$$\leq x_2^* Q x_2 \tag{C-13}$$

$$= x_2^* B^* \tilde{Q} B x_2 \tag{C-14}$$

(By (C-8) and (C-9))

$$= y^* (B B^\dagger) \tilde{Q} (B B^\dagger) y \tag{C-15}$$

$$= y^* \tilde{Q} y \tag{C-16}$$

which establishes claim b.

APPENDIX D

PROOF OF THEOREM 1

From the sector stability criterion,[1] it suffices to show that $\underset{\sim}{L}_{ev}$ outside

$$\text{Cone}\left(\underset{\sim}{Q}, \underset{\sim}{R}_c, \underset{\sim}{S}_c\right) \triangleq \text{sector} \begin{pmatrix} \underset{\sim}{S}_c & \underset{\sim}{R}_c \\ \underset{\sim}{S}_c & -\underset{\sim}{R}_c \end{pmatrix}$$

and that $\delta \underset{\sim}{C}$ inside Cone $(\underset{\sim}{Q}, \underset{\sim}{R}_c, \underset{\sim}{S}_c)$. The former follows from Lemma B (Appendix B). The latter follows from the composite sector property.[1]

---

[1] M. G. Safonov, "Robustness and Stability Aspects of Stochastic Multivariable Feedback Design," PhD Dissertation, MIT, September 1977.

APPENDIX E

PROOF OF THEOREM 2

The overall input-output relation $\underset{\sim}{T}$ of the system is

$$\underset{\sim}{T} = \underset{\sim}{L}_{yu} + L_{yv} \left((\delta \underset{\sim}{C})^I - L_{ev} \right)^I \underset{\sim}{L}_{eu} \tag{E-1}$$

We are given that for all i = 1, . . . , N

$$\delta \underset{\sim}{C} \text{ strictly inside Cone } (\underset{\sim}{O}, \underset{\sim}{R}_c, \underset{\sim}{S}_c) \tag{E-2}$$

From which it follows (from the proof of Theorem 1) that

$$\delta C_i \text{ inside sector } \begin{pmatrix} \underset{\sim}{S}_c & \underset{\sim}{R}_c \\ \underset{\sim}{S}_c & -\underset{\sim}{R}_c \end{pmatrix}$$

Applying the inverse, sum, inverse, and premultiplier sector properties, it follows that

$$\left((\delta \underset{\sim}{C})^I - \underset{\sim}{L}_{ev} \right)^I \underset{\sim}{L}_{eu} \text{ inside}$$

$$\text{Sector } \begin{pmatrix} \underset{\sim}{S}_c + \underset{\sim}{R}_c \underset{\sim}{L}_{ev} & \underset{\sim}{R}_c \underset{\sim}{L}_{eu} \\ \underset{\sim}{S}_c - \underset{\sim}{R}_c \underset{\sim}{L}_{ev} & -\underset{\sim}{R}_c \underset{\sim}{L}_{eu} \end{pmatrix} \tag{E-3}$$

Hence, for any input-output pair ($\underline{u}$, $\underline{v}$) satisfying

$$\underline{V} = \left(\delta \underset{\sim}{C} + \underset{\sim}{L}_{ev}\right)^{I} \underset{\sim}{L}_{eu}\, \underline{u} \tag{E-4}$$

We have

$$\langle(\underset{\sim}{S}_c + \underset{\sim}{R}_c\, \underset{\sim}{L}_{ev})\, \underline{v} + \underset{\sim}{R}_c\, \underset{\sim}{L}_{eu}\, \underline{u},\ (\underset{\sim}{S}_c - \underset{\sim}{R}_c\, \underset{\sim}{L}_{ev})\, \underline{v} + \underset{\sim}{R}_c\, \underset{\sim}{L}_{eu}\, \underline{u}\rangle$$

$$\leq 0 \tag{E-5}$$

Now, from conditions (a) and (b) and Theorem 1 (the multiloop circle theorem) the relation $((\delta \underset{\sim}{C})^{I} - \underset{\sim}{L}_{ev})^{I}$ is stable. Since by hypothesis L_{ev} is stable, it follows that $((\delta \underset{\sim}{C})^{I} - \underset{\sim}{L}_{ev})^{I}\, \underset{\sim}{L}_{eu}$ is stable and hence, whenever $\underline{u} \in L_2$ then $\underline{v} \in L_2$. For any u, $v \in L_2$ let $U(j\omega)$ and $V(j\omega)$ denote the respective fourier transforms of $\underline{u}$ and $\underline{v}$. From (B-5) and Parseval's theorem it follows that for all $\underline{u}$ L_2

$$0 \geq \int_0^{\infty} \left[\left((\underset{\sim}{S}_c + \underset{\sim}{R}_c \underset{\sim}{L}_{ev})\, \underline{v} + \underset{\sim}{R}_c \underset{\sim}{L}_{eu}\, \underline{u}\right)(t)\right]^{T}$$

$$\cdot \left[\left((\underset{\sim}{S}_c - \underset{\sim}{R}_c\, \underset{\sim}{L}_{ev})\, \underline{v} - \underset{\sim}{R}_c\, \underset{\sim}{L}_{eu}\, \underline{u}\right)(t)\right] \cdot dt \tag{E-6}$$

$$= \int_{-\infty}^{0} \left[\left(\underline{S}_c(j\omega) + \underline{R}_c(j\omega)\, \underline{L}_{eu}(j\omega)\right)\ \underline{V}(j\omega)\right.$$

$$\left. + \underline{R}_c(j\omega)\, \underline{L}_{eu}(j\omega)\, \underline{U}(j\omega)\right]$$

$$\cdot \left[\left(\underline{S}_c(j\omega) - \underline{R}_c(j\omega)\, \underline{L}_{ev}(j\omega)\right)\ \underline{V}(j\omega)\right.$$

$$- \underline{R}_c(j\omega)\,\underline{L}_{eu}(j\omega)\,\underline{U}(j\omega)\Big]\quad d\omega \tag{E-7}$$

$$= \int_{-\infty}^{\infty} \left[V^*(j\omega)\ U^*(j\omega)\right] \begin{bmatrix} P_v(j\omega) & -Z(j\omega) \\ -Z^*(j\omega) & -\theta(j\omega) \end{bmatrix} \begin{bmatrix} V(j\omega) \\ U(j\omega) \end{bmatrix} d \tag{E-8}$$

$$\int_{-\infty}^{\infty} \Big\{ \cdot \Big[V(j\omega) - T_v(j\omega)\ U(j\omega)\Big]^* Q_v(j\omega) \Big[V_{(j\omega)} - T_v(j\omega)\ U(j\omega)\Big]$$

$$- U^*(j\omega)\, R_T(j\omega)\, U(j\omega) \Big\}\, d\omega \tag{E-9}$$

where

$$Q_V(s) \triangleq S_c{}^T(-s)\, S_c(s) - L_{ev}(-s)\, R_c{}^T(-s)\, R_c(s)\, L_{ev}(s) \tag{E-10}$$

$$Z(s) \triangleq L_{ev}{}^T(-s)\, R_c{}^T(-s)\, R_c(s)\, L_{eu}(s) \tag{E-11}$$

$$\theta(s) \triangleq L_{eu}{}^T(-s)\, R_c{}^T(-s)\, R_c(s)\, L_{eu}(s) \tag{E-12}$$

$$T_V(s) \triangleq Q_V{}^{-1}(s)\, Z(s) \tag{E-13}$$

$$P_V(s) \triangleq \theta(s) + Z^T(-s)\, Q_V{}^{-1}(s)\, Z(s) \tag{E-14}$$

$$= (R_c(-s)\, L_{eu}(-s))^T \Big[I +$$

$$R_c(s)\, L_{ev}(s) \left(S_c^T(-s)\, S_c(s) - \left(R_c(-s)\, L_{ev}(-s) \right)^T \left(R_c(s)\, L_{ev} \right) \right)^{-1}$$

$$\cdot \left(R_c(-s)\, L_{ev}(-s) \right)^T \Big] R_c(s)\, L_{eu}(s) \qquad \text{(E-15)}$$

$$= L_{eu}^T(-s)\, R_c^T(-s) \Big[I - R_c(s)\, L_{ev}(s) \left(S_c^T(-s)\, S_c(s) \right)^{-1}$$

$$L_{ev}^T(-s)\, R_c^T(-s) \Big]^{-1} \cdot R_c(s)\, L_{eu}(s) \qquad \text{(E-16)}$$

$$\triangleq P_T(s)^{\dagger}$$

Thus, it follows that

$$\left|\left| \underset{\sim}{P}_T^{\frac{1}{2}}\, \underline{u} \right|\right|_{L_2}^2$$

$$= \int_{-\infty}^{\infty} U^*(j\omega)\, \underline{P}_T(j\omega)\, U(j\omega)\, d\omega \quad \text{(by Parseval's Theorem)}$$

---

†Note that in deducing (E-16) from (E-15), we have used the matrix identity

$$I + A(s) \left(B(s) - A^T(-s)\, A(s) \right)^{-1} A^T(s)$$

$$= \left[(I - A(s) \left(B(s) \right)^{-1} A^T(-s) \right]^{-1}$$

$$\geq \int_{-\infty}^{\infty} \left[V(j\omega) - T_v(j\omega)\, U(j\omega) \right]^* Q_v(j\omega) \left[V(j\omega) - T_v(j\omega)\, U(j\omega) \right] d\omega$$

(from (B-6)-(B-8))

$$\geq \int_{-\infty}^{\infty} \left[L_{yv}(V(j\omega) - T_v(j\omega)\, U(j\omega) \right]^* \left(L_{yv}^*(j\omega)\, Q_v^{-1}(j\omega)\, L_{yv}(j\omega) \right)^{-1}$$

$$\left[L_{yv}(j\omega)\, (V(j\omega) - T_v(j\omega)\, U(j\omega) \right] d\omega$$

(By Lemma C, Appendix C)

$$= \int_{-\infty}^{\infty} \left[\Delta Y^*(j\omega)\; U^*(j\omega) \right] \begin{bmatrix} \underline{I} \\ -\Delta T^*(j\omega) \end{bmatrix} Q_T(j\omega) \left[I - \Delta T(j\omega) \right] \begin{bmatrix} \Delta Y(j\omega) \\ U(j\omega) \end{bmatrix} d\omega$$

$$= \left\| \underset{\sim}{Q}_T^{\frac{1}{2}} \left(\Delta \underline{y} - \Delta T u \right) \right\|_{L_2}^2 \qquad \text{(E-18)}$$

(By Parseval's Theorem)

where

$$\Delta y \triangleq \underset{\sim}{L}_{yv}\, \underline{V}$$

$$\Delta \underline{T}(s) \triangleq \underline{L}_{yv}(s)\, \underline{T}_v(s) = \underline{L}_{yv}(s)\, Q_v^{-1}(s)\, \underline{Z}(s)$$

$$= L_{yv} \left(S_c^T(-s)\, S_c(s) - L_{ev}^T(-s)\, R_c^T(-s)\, R_c(s)\, L_{ev}(s) \right)^{-1}$$

$$\cdot\; L_{ev}^T(-s)\, R_c^T(-s)\, R_c(s)\, L_{eu}(s)$$

Since $\underline{y} = L_{yv}\,\underline{v} + Y_{yu}\underline{u} = \Delta\underline{y} + L_{yu}\,\underline{u}$, it follows from (E-18) that

$$\left\| P_T^{\frac{1}{2}}\,\underline{u} \right\|_{L_2}^2 \geq \left\| \underset{\sim}{Q}^{\frac{1}{2}}\,\underline{y} - (L_{yu} + \Delta T)\,\underline{u} \right\|_{L_2}^2$$

$$= \left\| \underset{\sim}{Q}^{\frac{1}{2}}\,(y - \underset{\sim}{T}_{nom})\,\underline{u} \right\|_{L_2}^2$$

(End of Proof)

APPENDIX F

PROOF OF THEOREM 3

We adopt the notation of Appendix E. Suppose $(u, y) \in L_2$-Cone $(\underset{\sim}{T}_{NOM}, \underset{\sim}{P}_T^{\frac{1}{2}}, \underset{\sim}{Q}_T^{\frac{1}{2}})$. Let $(U(j\omega), Y(j\omega))$ denote the Fourier transforms of $^*u, y)$. Let

$$V(j\omega) = L_{yv}^{+}(j\omega)(Y(j\omega) - L_{yu}(j\omega)\, U(j\omega) + T_v(j\omega)\, U(j\omega) \qquad \text{(F-1)}$$

where (suppressing $j\omega$'s)

$$L_{yv}^{+} = Q_v^{-1} L_{yv}^{*} \left[L_{yv}\, Q_v^{-1}\, L_{yv}^{*} \right]^{-1} \qquad \text{(F-2)}$$

is (refer to the proof of Lemma C) the pseudo-inverse of L_{yv} considered as a map of $C^n_{Q_v(j\omega)}$ into C^r_I. $^+$ Consequently (see the proof of Lemma C, (C-8 through (C-10)) it follows from the fact that L_{yv}^{+} maps into the orthogonal complements of the null space of L_{yv} (relative to the inner product space $C^n_{Q_v(j\omega)}$) that V is in the orthogonal complement of the null space of L_{yv} (again relative to $C^n_{Q_y}$). Hence, (see Eq. (C-8) through (C-10) in this proof of Lemma C), we have that

$$(V - T_v U)^{*} L_{yv}^{*} (L_{yv}\, Q_v^{-1}\, L_{yv}\, Q_v^{-1}\, L_{yv}^{*}) \qquad \text{(F-3)}$$

$$= (V - T_v U)^{*} Q_v (V - T_v U)$$

This fact will be used shortly.

Now, since (y, u) inside cone ($\underset{\sim}{T}_{NOM}$, $\underset{\sim}{P}_T^{\frac{1}{2}}$) we have from Parseval's Theorem that:

$$0 \leq \int_{-\infty}^{\infty} dw \left(\| P_T^{\frac{1}{2}} U \|^2 - \| G_T^{\frac{1}{2}} (Y - T_{NOM} U \|^2 \right) \quad \text{(F-4)}$$

$$= \int_{-\infty}^{\infty} dw \left(\| P_T^{\frac{1}{2}} U \|^2 - \| Q_T^{\frac{1}{2}} L_{yv} (V - T_v U) \|^2 \right) \quad \text{(F-5)}$$

$$= \int_{-\infty}^{\infty} dw \left(\| P_T^{\frac{1}{2}} U \|^2 - (V - T_v U)^* L_{yv} Q_v L_{yv}^*) L_{yv} \cdot (V - T_v U) \right) \quad \text{(F-6)}$$

Then clearly $\delta \underset{\sim}{C}$ inside Cone (O, R_e, S_e) since

$$\| \underset{\sim}{S}^{\delta} \underset{\sim}{C} z \|_{L2} = \left(\frac{\langle R_c e, R_c z \rangle_{L_2}}{\| R_c e \|^2_{L_2}} \right)$$

$$\leq \frac{\| R_c e \|_{L_2} \| R_c z \|_{L_2} \| S_{cv} \|_{L_2}}{\| R_c e \|^2_{L_2}}$$

(By the Schwartz inequality)

$$= \frac{\| R_c z \|_{L_2} \| S_c v \|_{L_2}}{\| R_c e \|_2}$$

$$\leq \| R_c z \|$$

Since (e, v) inside L_2 - Cone (O, R, S)). And further

$$\delta \underset{\sim}{C}\, e = V$$

$$= \int_{-\infty}^{\infty} dw \left(U^{*} P_T U - (V - T_v U)^{*} Q_v (V - T_v U) \right)$$

From (F-3)

$$= \int_{-\infty}^{\infty} - \left[(\underset{\sim}{S}_c + \underset{\sim}{R}_c \underset{\sim}{L}_{ev}) v + \underset{\sim}{R}_c \underset{\sim}{L}_{cv} \underline{u}) (t) \right]^T$$

$$\left[(\underset{\sim}{S}_c - \underset{\sim}{R}_c \underset{\sim}{L}_{ev}) v - \underset{\sim}{R}_c \underset{\sim}{L}_{eu} \underline{u}) (t) \right] \quad dt$$

(See Eq. (E-6) through (E-9) of Appendix E)

$$= \int_{-\infty}^{\infty} - \left[(\underset{\sim}{S}_c \underline{v} + \underset{\sim}{R}_c e)(t) \right]^T \left[(\underset{\sim}{S}_c v - \underset{\sim}{R}_c \underline{e}) (t) \right] \quad dt$$

(since $\underset{\sim}{L}_{eu} \underline{u} + \underset{\sim}{L}_{ev} \underline{v} = \underline{e}$)

$$= - \| \underset{\sim}{S}_c \underline{v} \|^2_{L_2} + \| \underset{\sim}{R}_c e \|^2_{L_2}$$

Hence,

(e, v) inside Cone ($\underset{\sim}{O}$, $\underset{\sim}{R}_c$, $\underset{\sim}{S}_c$)

Let $\underset{\sim}{SC}$ be the mapping defined by

$$(\delta \underset{\sim}{C} z)(t) = \left(\frac{< \underset{\sim}{R}_c e, \underset{\sim}{R}_c z >}{\| \underset{\sim}{R}_c \underline{e} \|} \right) \cdot v(t)$$

APPENDIX G

LEMMA D

Let $\hat{Q}$, $\hat{R}_s$, $\hat{E}_s$, $\hat{\theta}_s$ and S be as in Section 3 of the main report and suppose that there exists an $\hat{S}_o \epsilon S$ such that Eq. (127)-(128) are satisfied. Then $\hat{S}_o$ is a global minimum of $J_1(S)$,

$$J_1(\hat{S}_o) = 0$$

and $J_1(\hat{S})$ has no local minimum $\hat{S}_1$ with $J_1(\hat{S}) > 0$.

PROOF

From Eq. (127) - (128) we readily verify that $J_1(S) \geq 0 \; \forall \; S$ and $J_1(S_o) = 0$. So S_o is clearly a global minimum of $J_1(S)$.

It remains to prove $J_1(\hat{S})$ has no local minimum $\hat{S}_1$ with $J_1(\hat{S}_1) > 0$. For the sake of argument suppose $\hat{S}_1$ is a local minimum of $J_1(S)$ with $J_1(S_1) > 0$. Since every element of $\hat{S}$ is stable and rational it follows that

$$\|\hat{S}_1 - \hat{S}_o\| \triangleq \sup_{\omega} \sigma_{max}(\hat{S}_1 - \hat{S}_o) < \infty.$$

From[1] (Lemma C) it follows that

$$\hat{S}_2 = \delta \cdot \hat{S}_o + (1-\delta) \cdot \hat{S}_1 \epsilon S$$

---

[1] D. C. Youla, et al., "Modern Wiener-Hopf Design of Optimal Controllers--Part II: The Multivariable Case," IEEE Trans. On Automatic Control, Vol. AC-21, 1976, pp. 319-338.

(except possibly for at most $p \triangleq \dim(y)$ distinct values of $\delta \epsilon R$). Hence for every $\epsilon > 0$ there exists a $\delta > 0$ such that $\hat{S}_2 = \delta \cdot \hat{S}_o + (1 - \delta) \cdot \hat{S}_1 \epsilon S$ and

$$||\hat{S}_2 - \hat{S}_1|| = \delta \cdot ||\hat{S}_o - \hat{S}_1|| < \epsilon$$

Now, using the fact that Eq. (135) holds, the expression (132) for $J_1(\hat{S})$ can be rewritten as

$$J_1(S) = \frac{1}{2\pi} \int_{-\infty}^{\infty} \sum_{1=1}^{p} \left\{ \hat{\alpha}_1 \cdot \sigma_i^2 \left(\hat{Q}_s^{\frac{1}{2}(r)} \hat{S} \hat{\Xi}_s^{\frac{1}{2}(\ell)} \right) \cdot \delta_{-1} \left(\sigma_i^2 (\hat{Q}_s^{\frac{1}{2}(r)} \cdot \hat{S} \cdot \hat{\Xi}^{\frac{1}{2}(\ell)} - 1) \right) + \alpha_2 \cdot \sigma_i^2 \left(R_s^{\frac{1}{2}(r)} (I - \hat{S}) \cdot \hat{\theta}_s^{\frac{1}{2}(\ell)} \right) \cdot \delta_{-1} \left(\sigma_i^2 (\hat{R}_s^{\frac{1}{2}(r)} \cdot (I - \hat{S}) \cdot \hat{\theta}_s^{\frac{1}{2}(\ell)}) - 1 \right) \right\} d\omega$$

From Lemma E, it follows that

$$J_1(\hat{S}_2) < J_1(\hat{S}_1)$$

contradicting the hypothesis that $\hat{S}_1$ is a local minimum of $J_1(S)$ with $J(S_1) > 0$. Q.E.D.

LEMMA E

Let $X_o, X_1 \epsilon C^{pxp}$, let $\sigma_{max}(X_o) < 1$, let $\delta \epsilon [0, 1]$, and let

$$X_2 = (1 - \delta) \cdot X_1 + \delta \cdot X_2$$

Then

$$\sum_{i=1}^{p} \sigma_i^2(X_2) \, \delta_{-1}(\sigma_i^2(X_2) - 1)$$

$$< \sum_{i=1}^{p} \sigma_i^2(X_1)\delta_{-1}(\sigma_i^2(X_1) - 1$$

Proof: Let $a \epsilon C^p$ and consider the function $f: C^{pxp} \to R$ defined by

$$f(X) = a^* X X^* a$$

The second differential of f(X) is

$$2a \cdot \Delta X \cdot (\Delta X)^* a \geq 0$$

hence f(X) is a convex function; that is,

$$a^* X_2 X_2^* a \leq (1 - \delta)\, a^* X_1 X_1^* a + \delta\, a^* X_o X_o^2 a$$

for all $\delta \epsilon [0, 1]$ and all $a \epsilon C^p$.

Since the vector $\underline{a}$ is arbitrary it follows that

$$X_2 X_2^* \leq (1 - \delta) \cdot X_1 X_1^* + \delta \cdot X_o X_o^*$$

and therefore

$$X_2X_2^* \leq (1 - \delta) \cdot X_1X_1^* + \delta \cdot \sigma_{max}^2(X_o) \cdot I$$

Hence, denoting by $\lambda_i(AA^*) \triangleq \sigma_i^2(A)$ the ith eigenvalue of AA^* ordered according to size from largest to smallest (i.e., $\lambda(AA^*) > \lambda_2(AA^*) > \ldots \geq \lambda_p(AA^*)$), it follows from the above inequality that†

$$\lambda_i(X_2X_2^*) \leq \lambda_i((1 - \delta)X_1X_1^* + \delta \cdot \sigma_{max}^2(X_o) \cdot I)$$

$$= (1 - \delta)\, \lambda_i(X_1X_1^*) + \delta \cdot \sigma_{max}^2(X_o)$$

or equivalently,

$$\sigma_i^2(X_2) \leq (1 - \delta)\, \sigma_i^2(X_1) + \delta \cdot \sigma_{max}^2(X_o), \quad \forall\, i$$

It follows that $\forall i = 1, \ldots, p$

$$\sigma_i^2(X_2) \cdot \delta_{-1}(\sigma_i^2(X_2) - 1) \leq \left(\frac{1 - \delta}{1 - \delta \cdot \sigma_{max}^2(X_o)}\right) \sigma_i^2(X_1) \cdot \delta_{-1}(\sigma_i^2(X_1) - 1)$$

---

† The following brief proof was provided by J. C. Doyle:
Let m_i denote the set of all vector subspaces of dimension i. Suppose $A - B > 0$. Then

$$\lambda_i(A) = \max_{\text{Mem}_i} \left(\min_{x \in M} \frac{x^* Ax}{x^* x} \right)$$

$$= \max_{\text{Mem}_i} \left(\min_{x \in M} \frac{x^*(A - B)x}{x^* x} + \frac{x^* Bx}{x^* x} \right)$$

$$= \max_{\text{Mem}_i} \left(\min_{x \in M} \frac{x^* Bx}{x^* x} = \lambda_i(B) \right)$$

and since $\sigma_{max}(X_o) < 1$,

$$\sum_{i=1}^{p} \sigma_i^2(X_2) \cdot \delta_{-1} (\sigma_1^2(X_2) - 1)$$

$$< \sum_{i=1}^{p} \sigma_i^2(X_1) \cdot \delta_{-1} (\sigma_i^2(X_1) - 1)$$

Q. E. D.

DISTRIBUTION LIST

Office of Naval Research
800 N. Quincy St.
Arlington, VA 22217
R. von Husen, Code 211 — 4
S. L. Brodsky, Code 432 — 1

Office of Naval Research
Eastern/Central Regional Office
495 Summer St.
Boston, MA 02210 — 1

Office of Naval Research
Western Regional Office
1030 E. Green St.
Pasadena, CA 91106 — 1

Naval Research Laboratory
Washington, DC 20375
Code 2627 — 3

Naval Air Systems Command
Washington, DC 20361
D. Kirkpatrick, AIR 320D — 1
R. C. A'Harrah, AIR 53011 — 1

Naval Air Development Center
Warminster, PA 19874
C. J. Mazza, Code 6053 — 1
C. R. Abrams, Code 6072 — 1

Naval Material Command
Washington, DC 20360
Code 08T23 — 1

Naval Weapons Center
China Lake, CA 93555
B. Hardy, Code 3914 — 1

Naval Surface Weapons Center
Silver Spring, MD 20910
J. Wingate, Code R44 — 1

Naval Air Test Center
Patuxent River, MD 20670
J. McCue, Code TPS — 1

Naval Coastal Systems Center
Hydromechanics Division
Panama City, FL 32407
D. Humphreys, Code 794 — 1

David Taylor Naval Ship R&D Center
Bethesda, MD 20084
J. P. Feldman, Code 1564 — 1
W. E. Smith, Code 1576 — 1

Naval Post Graduate School
Monterey, CA 93940
Technical Reports Library — 1
L. Schmidt — 1
D. Kirk — 1

Defense Technical Information Center
Building 5
Cameron Station
Alexandria, VA 22314 — 12

Air Force Office of Scientific Research
Building 410
Bolling Air Force Base
Washington, DC 20332
G. W. McKemie — 1

Air Force Flight Dynamics Laboratory
Wright-Patterson Air Force Base
Dayton, OH 45433
R. Anderson, Control Dyn. Br. — 1
F. George, Control Dyn. Br. — 1

Air Force Institute of Technology
Wright-Patterson Air Force Base
Dayton, OH 45433
P. Maybeck — 1

Army Armament R&D Command
Building #18
Dover, NJ 07801
N. Coleman, DRDAR-SCFCC — 1

NASA Langley Research Center
Hampton, VA 23665
Technical Library — 1

NASA Dryden Research Center
P. O. Box 273
Edwards, CA 93523
Technical Library 1

National Transportation Safety Board
Bureau of Technology
Laboratory Services Division
800 Independence Ave., SW
Washington, DC 20 94
R. von Husen 1

Systems Technology, Inc.
13766 South Hawthorne Blvd.
Hawthorne, CA 90250
R. Whitbeck 1

The Analytic Sciences Corp.
6 Jacob Way
Reading, MA 01867
C. Price 1

Massachusetts Institute of Technology
Lab. for Information and Decision Systems
Cambridge, MA 02139
M. Athans 1

University of Michigan
Dept. of Naval Architecture & Marine Engr.
Ann Arbor, MI 48109
M. G. Parsons 1

Nielsen Engineering & Research, Inc.
510 Clyde Avenue
Mountain View, CA 94043
J. N. Nielsen 1

University of Notre Dame
Dept. of Electrical Engineering
Notre Dame, IN 46556
M. K. Sain 1

The C. S. Draper Laboratory, Inc.
555 Technology Square
Cambridge, MA 02139
R. V. Ramnath 1

Alphatech, Inc.
3 New England Executive Park
Burlington, MA 01803
N. R. Sandell 1

Scientific Systems, Inc.
Suite No. 309-310
186 Alewife Brook Parkway
Cambridge, MA 02138
R. K. Mehra 1

Calspan Corp.
P. O. Box 400
Buffalo, NY 14225
E. G. Rynaski 1
K. S. Govindaraj 1

Systems Control Inc.
1801 Page Mill Road
Palo Alto, CA 94306
E. Hall 1

Flight Research Laboratory
Dept. of Mechanical & Aerospace Engineering
Princeton University
Princeton, NJ 08544
R. F. Stengel 1